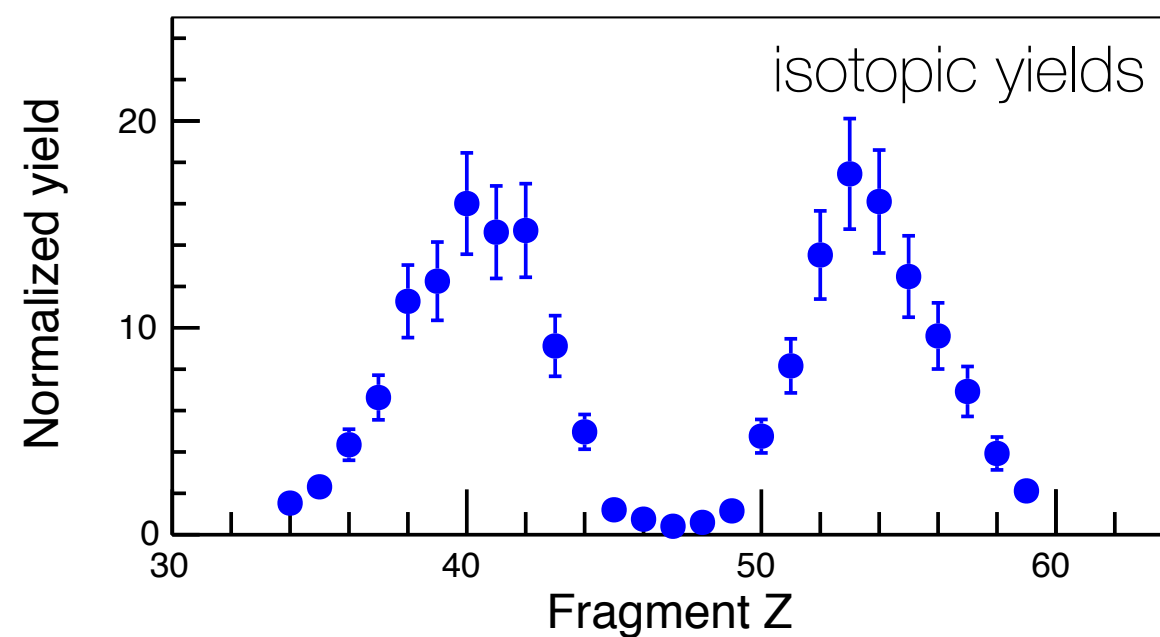
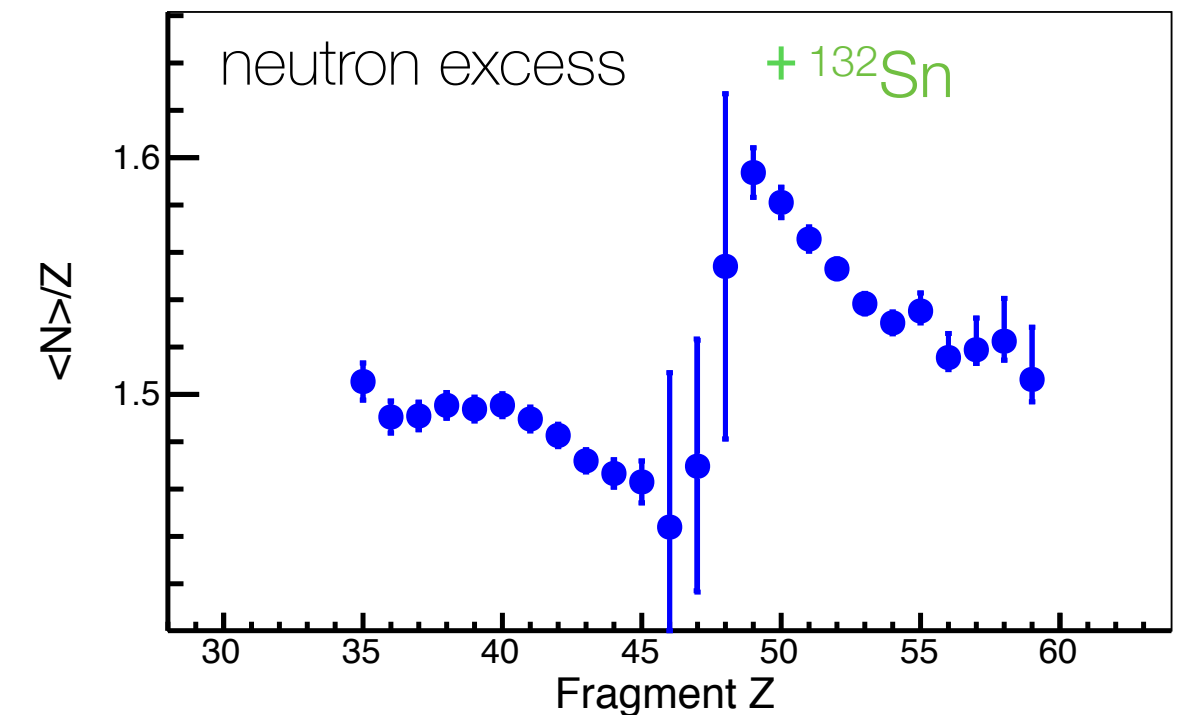
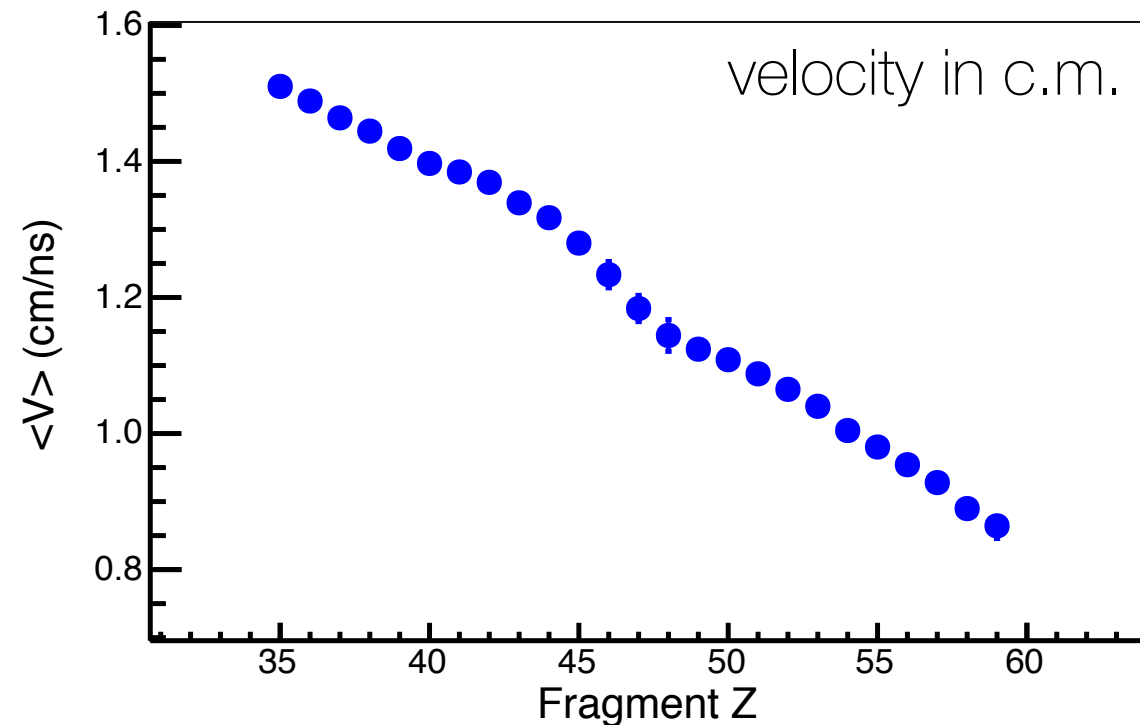


# Energetics and deformation at scission

M. Caamaño  
(U. Santiago de Compostela, Spain)

# Experimental observables

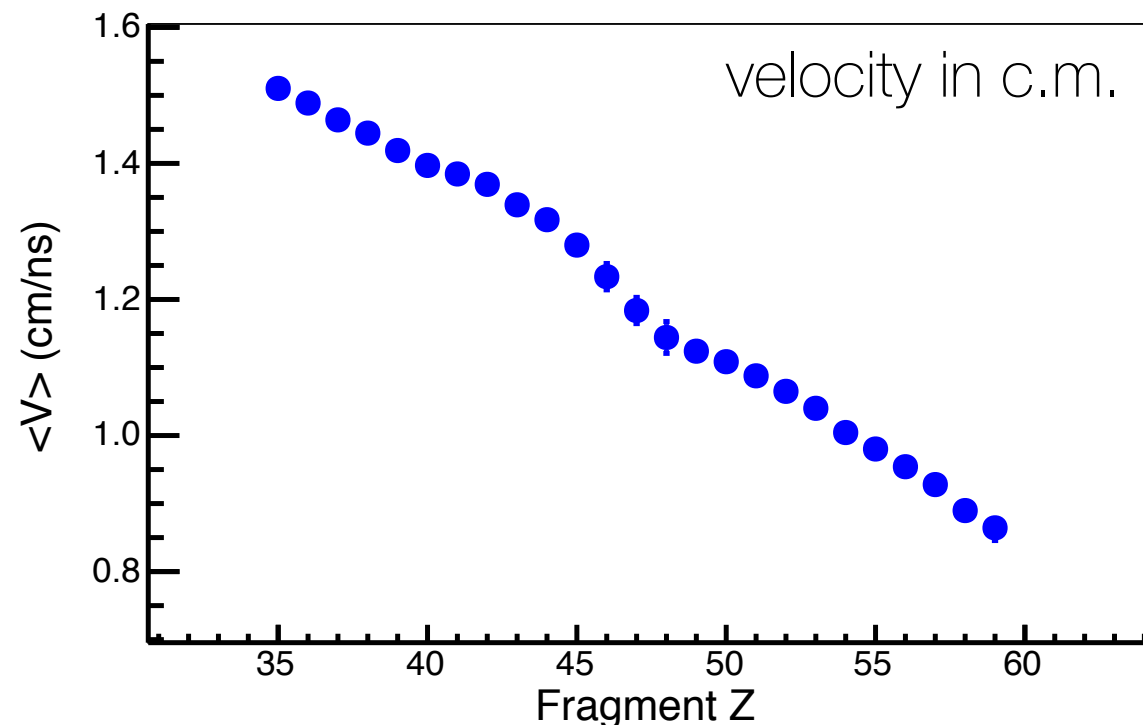


M. Caamaño, F. Farget et al., PRC 88, 024605 (2013)

Can we go further  
with simple assumptions?

We focus on  $^{240}\text{Pu}$  (  $\langle E^* \rangle = 9 \text{ MeV}$  )

# Experimental observables. Back to scission



$$\frac{\langle A^* \rangle_{Z1}}{\langle A^* \rangle_{Z2}} \approx \frac{\langle \beta\gamma \rangle_{Z2}}{\langle \beta\gamma \rangle_{Z1}}$$

C. Britt *et al.* NIM 24 (1963) 13

masses

$$\langle A^* \rangle_{Z1} \left( 1 + \frac{\langle \beta\gamma \rangle_{Z1}}{\langle \beta\gamma \rangle_{Z2}} \right) = A_{\text{FS}} - \langle \nu^{\text{pre}} \rangle$$

GEF code:  
K.-H. Schmidt *et al.*  
NDS 131,107 (2016)

total kinetic energy

$$TKE^* = u \langle A_1^* \rangle (\langle \gamma_1^* \rangle - 1) + u \langle A_2^* \rangle (\langle \gamma_2^* \rangle - 1)$$

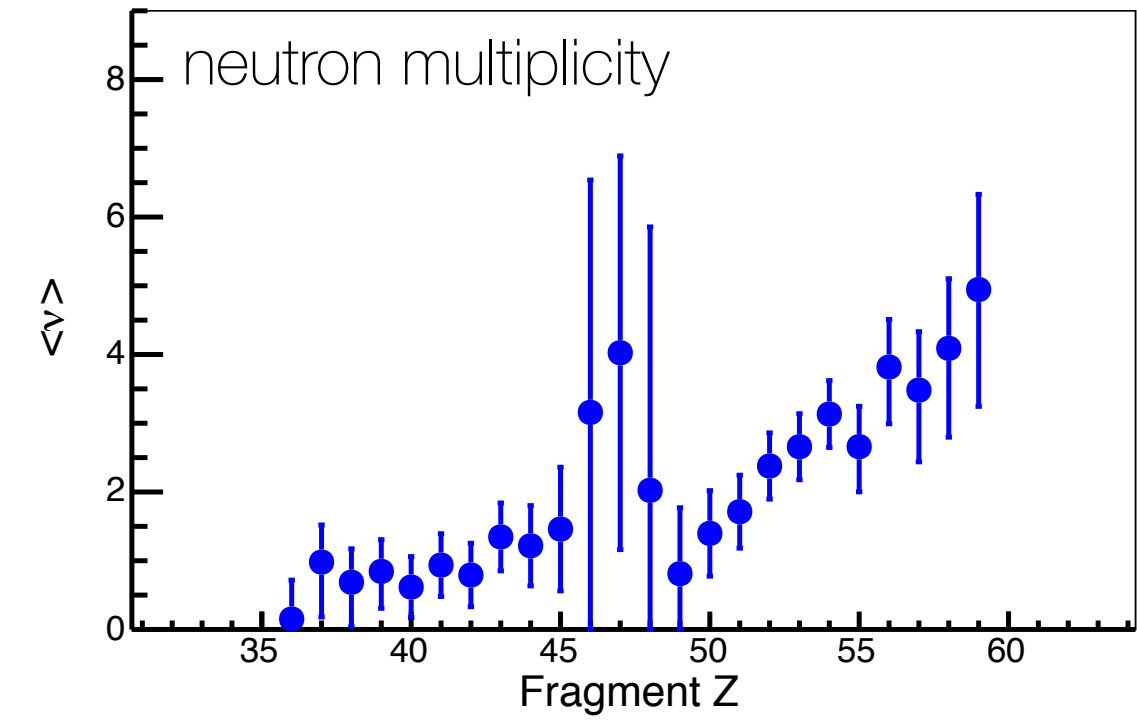
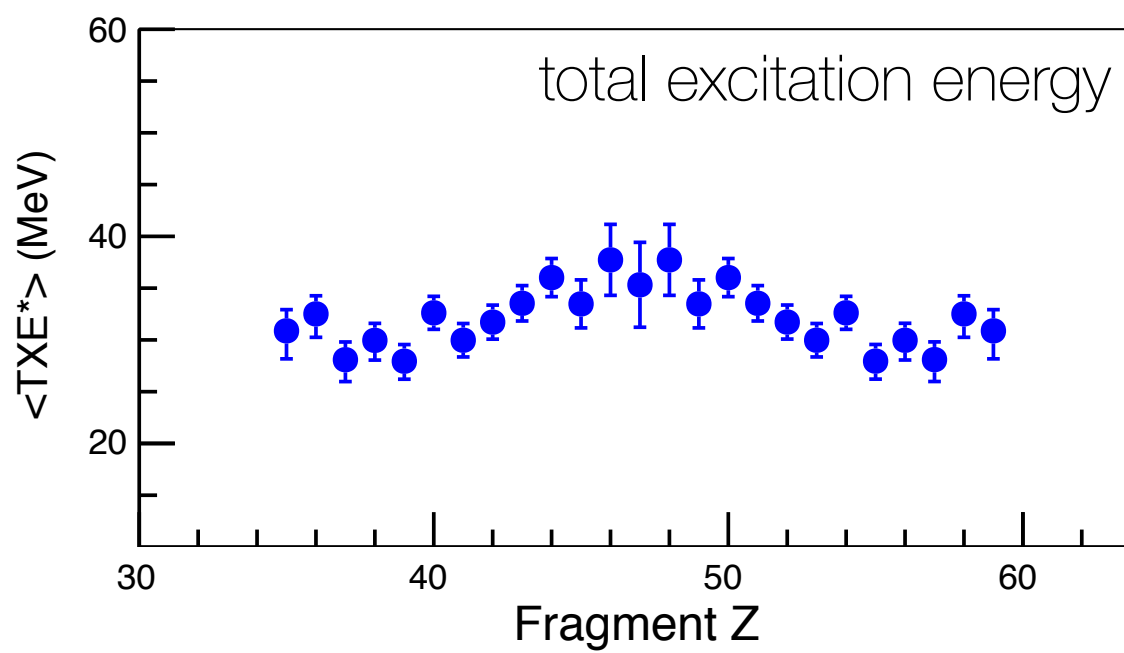
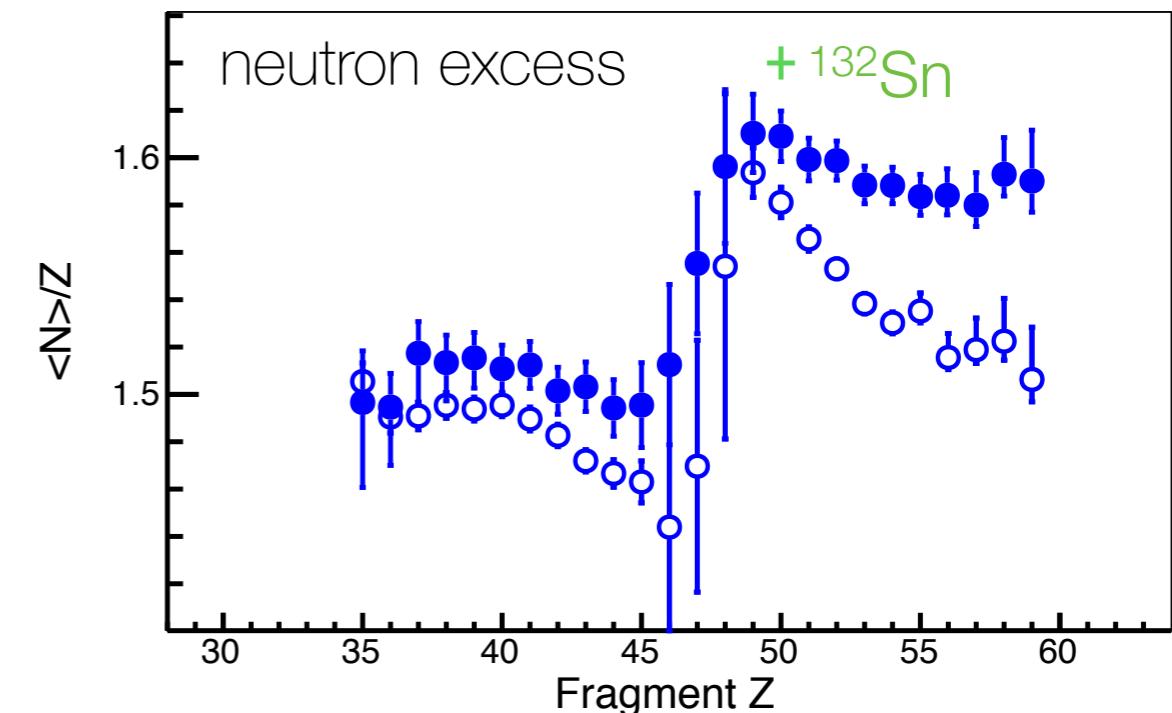
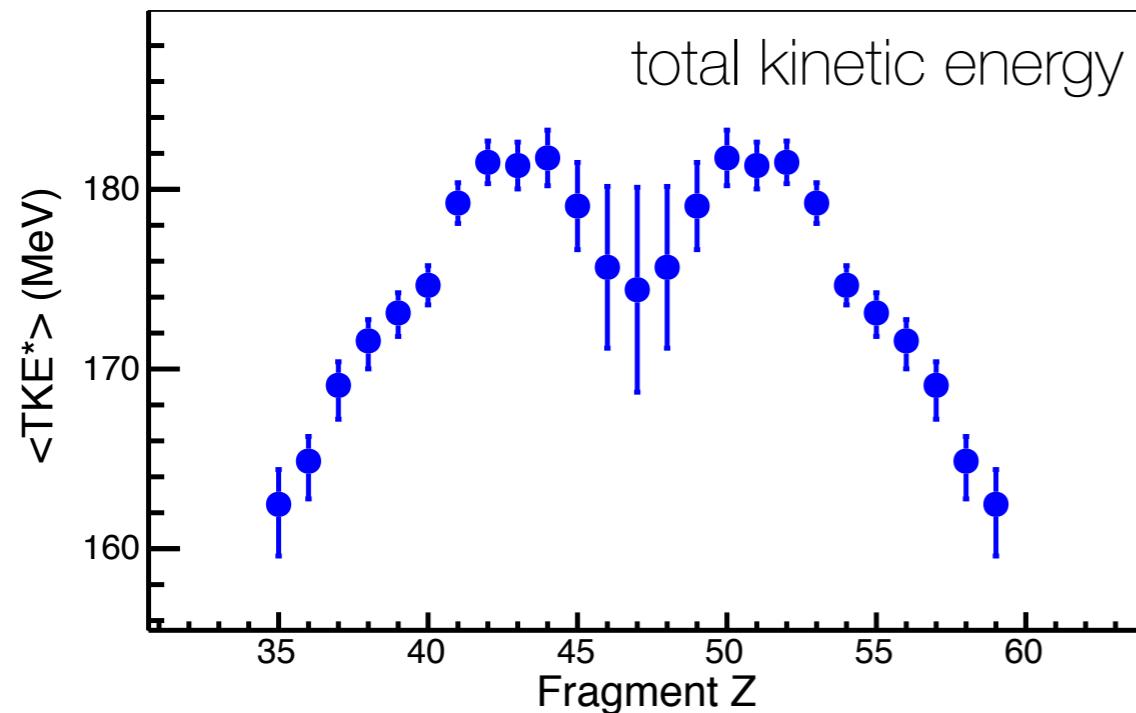
neutron multiplicity

$$\langle \nu \rangle_Z = \langle A^* \rangle_Z - \langle A^{\text{measured}} \rangle_Z$$

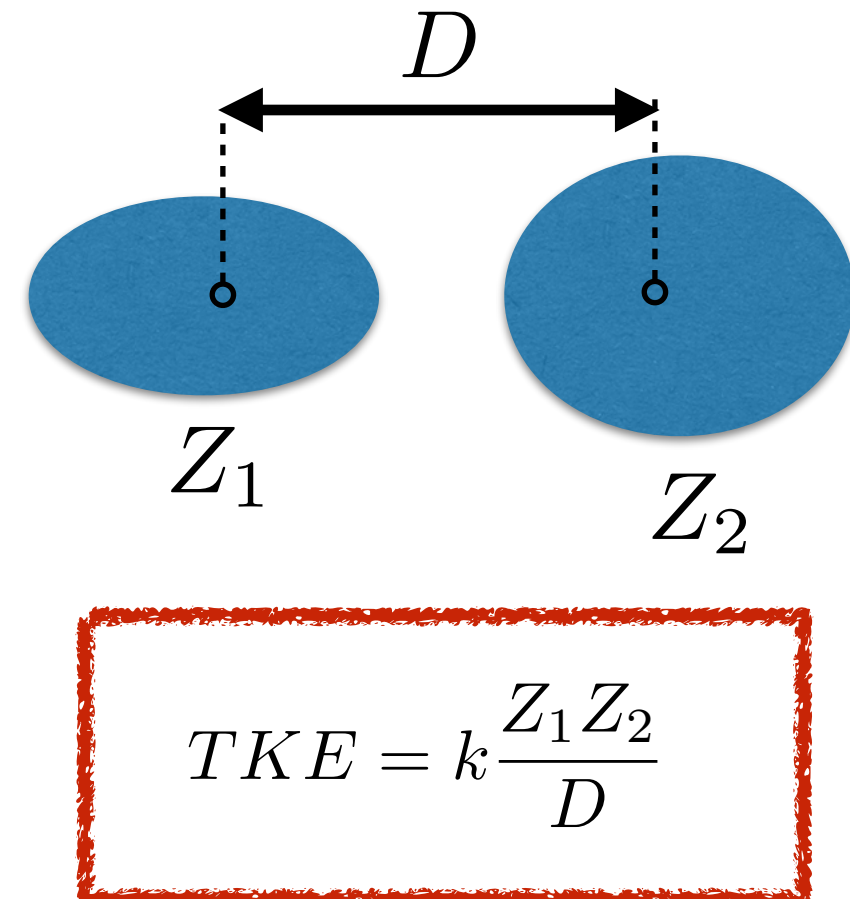
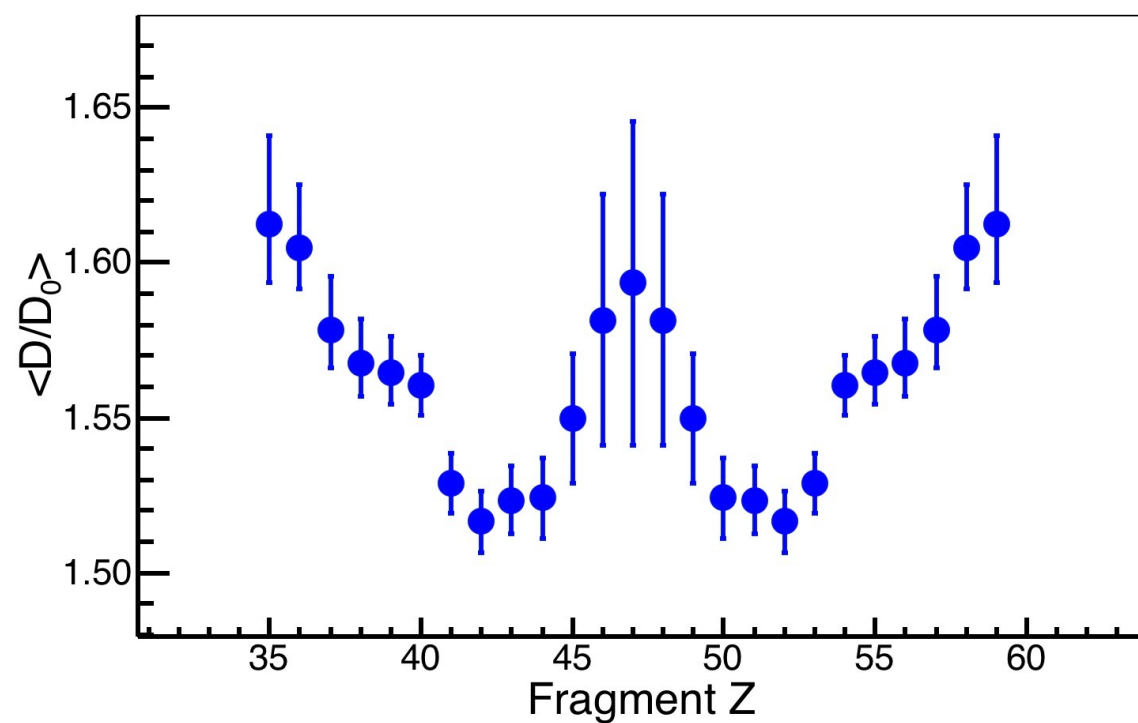
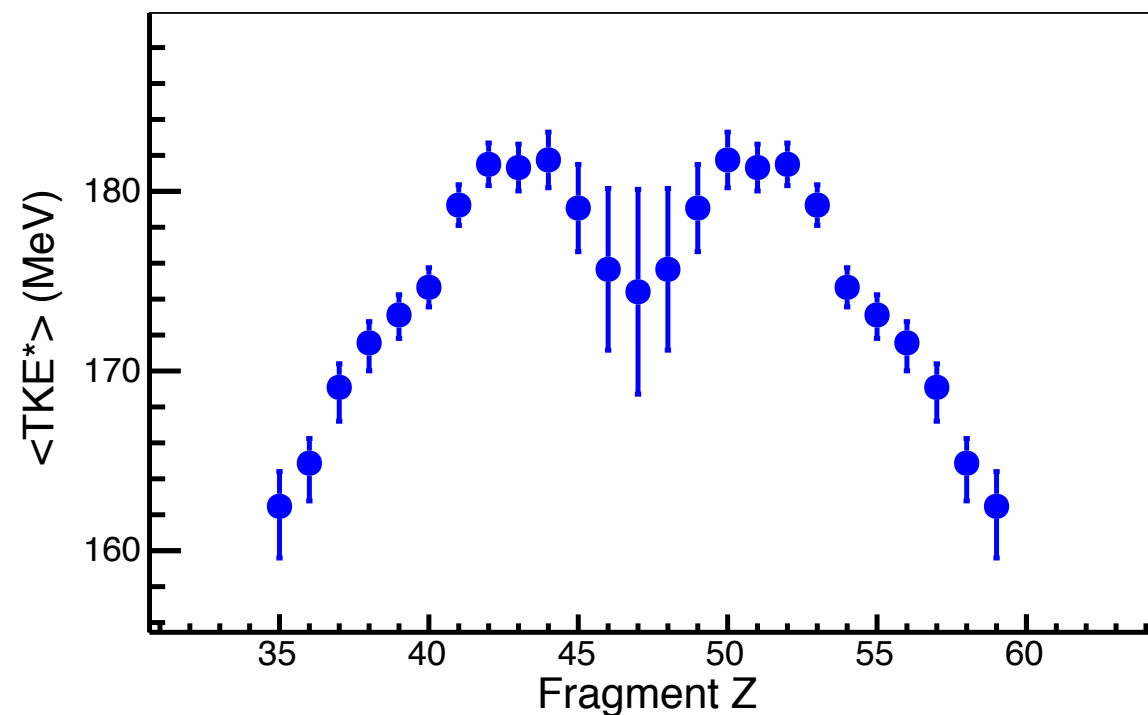
total excitation energy

$$\langle TXE^* \rangle = [M_{\text{FS}} + E_{\text{FS}}^*] - [\langle M_1^* \rangle + \langle M_2^* \rangle + \langle TKE^* \rangle]$$

# Experimental observables at scission



# Elongation at scission



A schematic diagram showing two spherical fragments,  $Z_1$  and  $Z_2$ , separated by an initial distance  $D_0$ . The fragments are represented by blue circles with white centers.

$$\frac{D}{D_0} = k \frac{Z_1 Z_2}{TKE} \frac{1}{r_0 A_1^{1/3} + r_0 A_2^{1/3}}$$

M. Caamaño, F. Farget et al., PRC 92, 034606 (2015)

## Energy balance at scission

Can we do more?

$$M_{\text{FS}} + E_{\text{FS}}^* = M_1 + M_2 + TKE + TXE$$

$$TKE = E^{k,C}(Z_1, Z_2, \beta_1, \beta_2, d) + E^{\text{k,pre}}$$

*Coulomb repulsion*      *fragment deformation & distance*      *pre-scission energy*

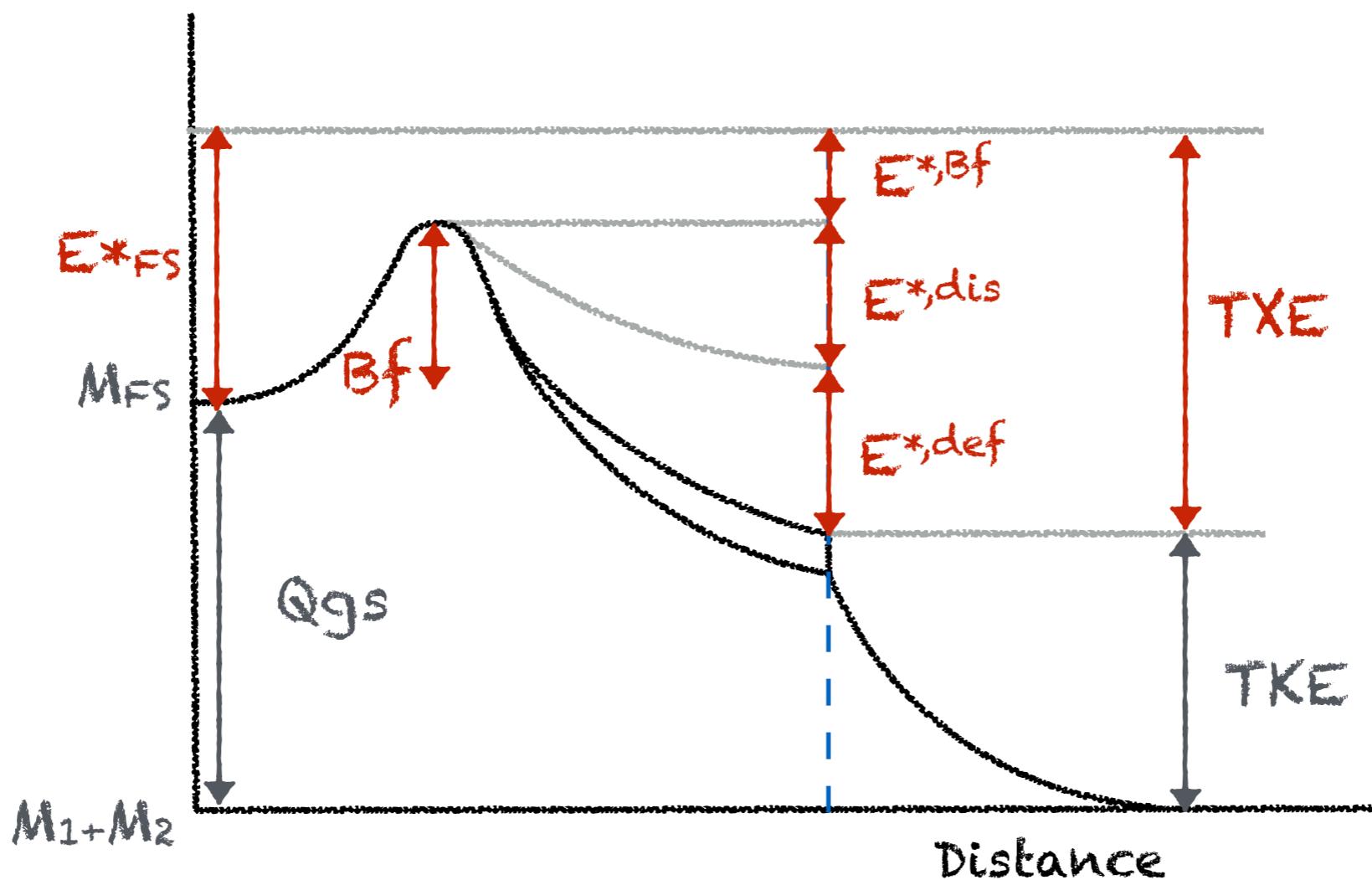
$$TXE = E^{*,\text{Bf}} + E^{*,\text{dis}} + \sum_{i=1}^2 E_i^{*,\text{def}}(\beta_i)$$

*energy above Bf*      *energy dissipated*      *deformation energy*

## Energy balance at scission. Excitation energy

$$TXE = E^{*,\text{Bf}} + E^{*,\text{dis}} + \sum_{i=1}^2 E_i^{*,\text{def}}(\beta_i)$$

energy above Bf      energy dissipated       $i=1$  deformation energy



## Energy balance at scission. Excitation energy

$$TXE = E^{*,\text{Bf}} + E^{*,\text{dis}} + \sum_{i=1}^2 E_i^{*,\text{def}}(\beta_i)$$

energy      energy       $i=1$  deformation  
 above Bf    dissipated      energy

The measurements of the  $E^*_{\text{FS}}$  of the fissioning system and its barrier are performed with the same setup

$$E^{*,\text{Bf}} = E^*_{\text{FS}} - \text{Bf} \approx 3 \text{ MeV}$$

C. Rodríguez Tajes et al., PRC 89, 025614 (2014)

The proton even-odd effect ( $\delta_z$ ) is related with the amount of intrinsic energy

$$E^{*,\text{Bf}} + E^{*,\text{dis}} \approx -4 \ln(\delta_z)$$

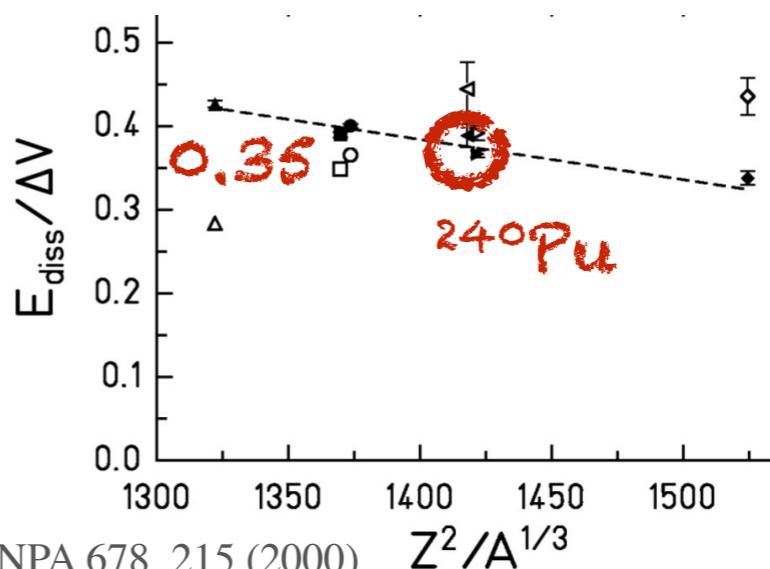
F. Gönnenwein, "The Nuclear Fission Process" (1991)

The dissipated energy can be also related with the available TXE:

$$E^{*,\text{dis}} = F^{\text{dis}}(TXE - E^{*,\text{Bf}})$$

$$F^{\text{dis}} \approx 0.35$$

GEF code: NDS 131,107 (2016)



F. Rejmund et al., NPA 678, 215 (2000)

## Energy balance at scission. Excitation energy

$$\sum_{i=1}^2 E_i^{*,\text{def}}(\beta_i) = (1 - F^{\text{dis}})(TXE - 3)$$

We need to split it between the fragments

This energy is released in post-scission evaporation:

$$TXE = \sum_{i=1}^2 Q_i^\nu + \nu_i \langle E^\nu \rangle + E_i^\gamma$$

measured      measured  
neutrons    neutrons    gamma  
binding E    kinetic E    emission

$$Q_i^\nu = M_i - \nu_i m_n - M_i^{\text{post}}$$

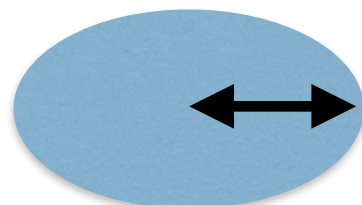
We assume that the sharing of the energy released is very similar to that of neutron binding

$$\frac{Q_1^\nu}{Q_2^\nu} \approx \frac{Q_1^\nu + \nu_1 \langle E_1^\nu \rangle + E_1^\gamma}{Q_2^\nu + \nu_2 \langle E_2^\nu \rangle + E_2^\gamma}$$

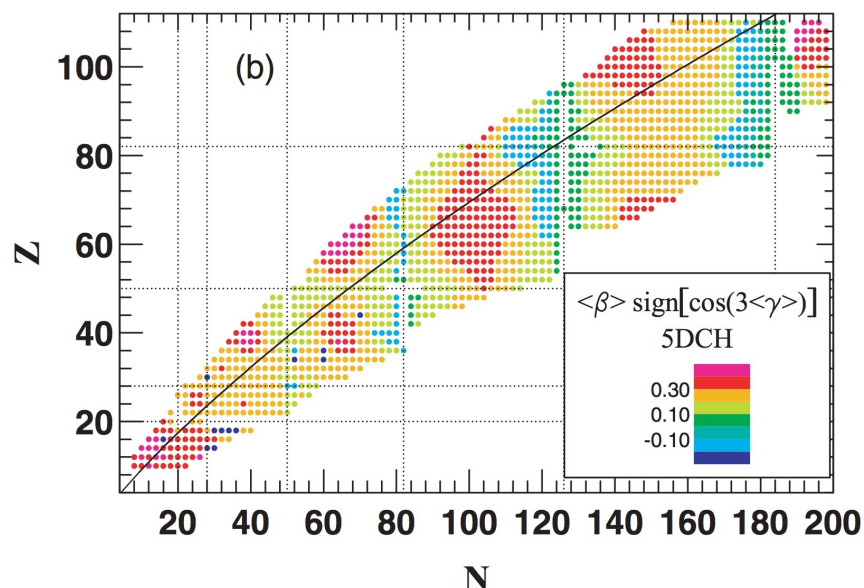
# Energy balance at scission. Excitation energy

$$E_i^{*,\text{def}}(\beta_i) \approx (1 - F^{\text{dis}})(TXE - 3) \left( \frac{Q_i^\nu}{Q_1^\nu + Q_2^\nu} \right)$$

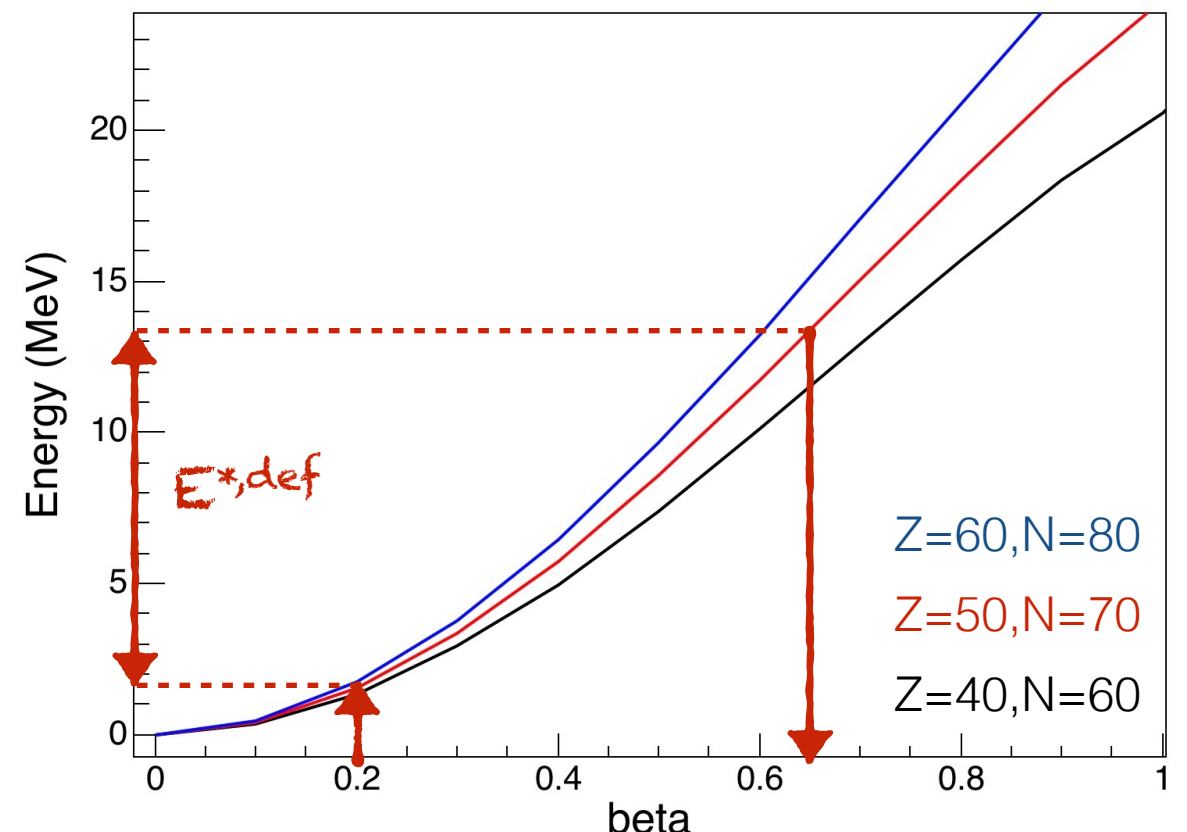
We transform the  $E_i^{*,\text{def}}$  into deformation with a simple factorisation around  $\beta$  of the mass formula, taking into account the deformation at the g.s.



$$r_{\text{major}} = r_0 A^{\frac{1}{3}} \left( 1 + \frac{2}{3} \beta \right)$$



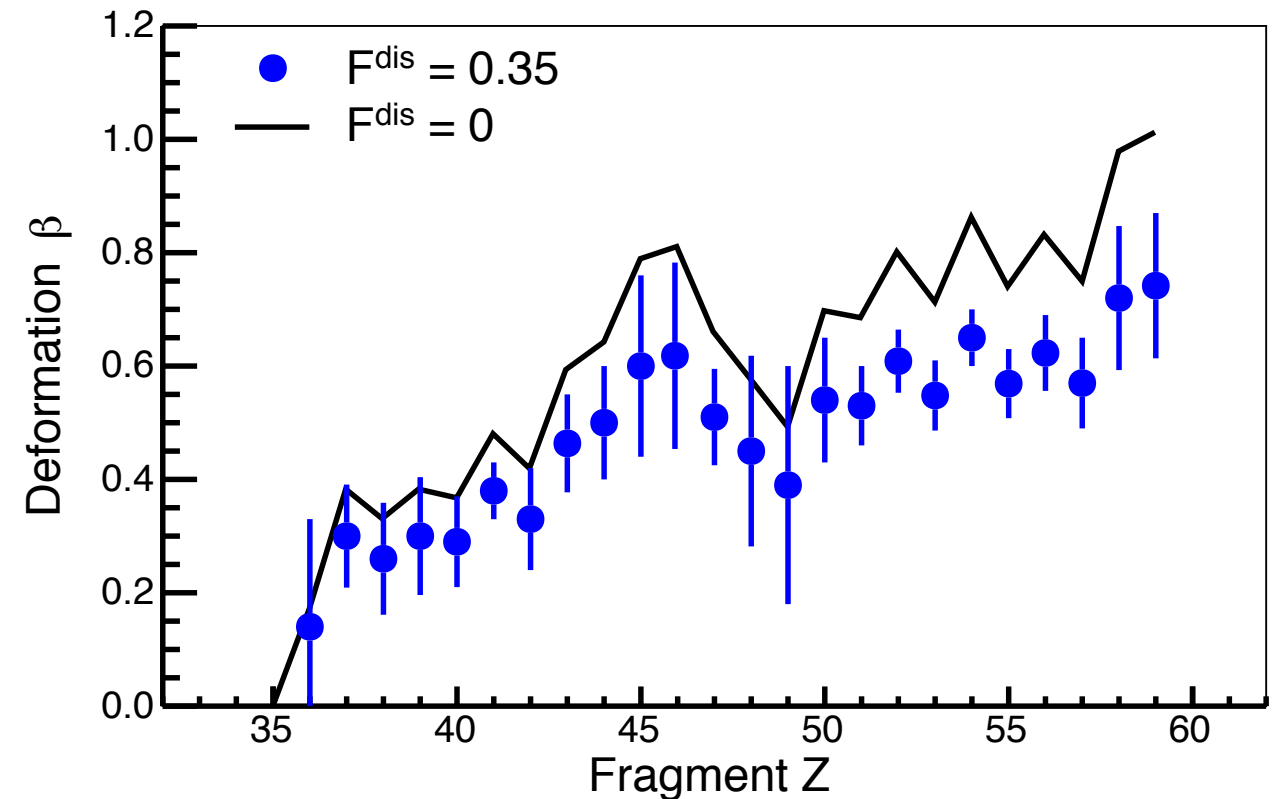
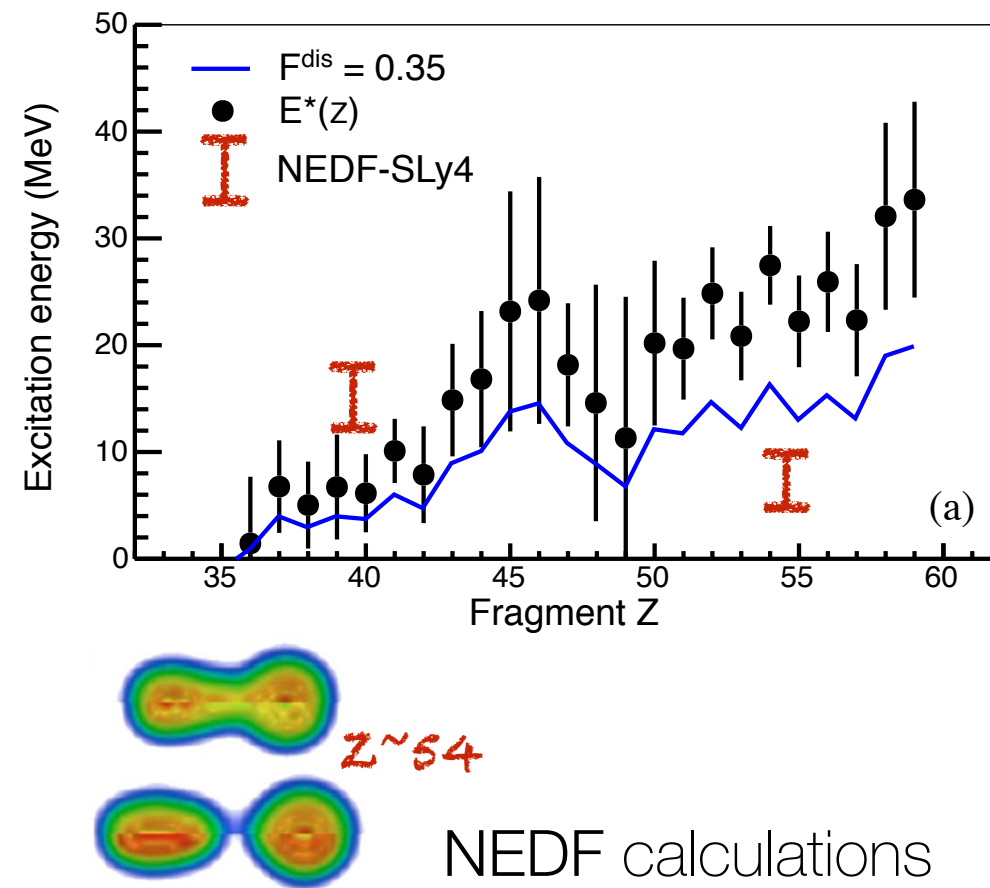
J.-P. Delaroche et al., PRC 81, 014303 (2010)



# Energy balance at scission. Deformation

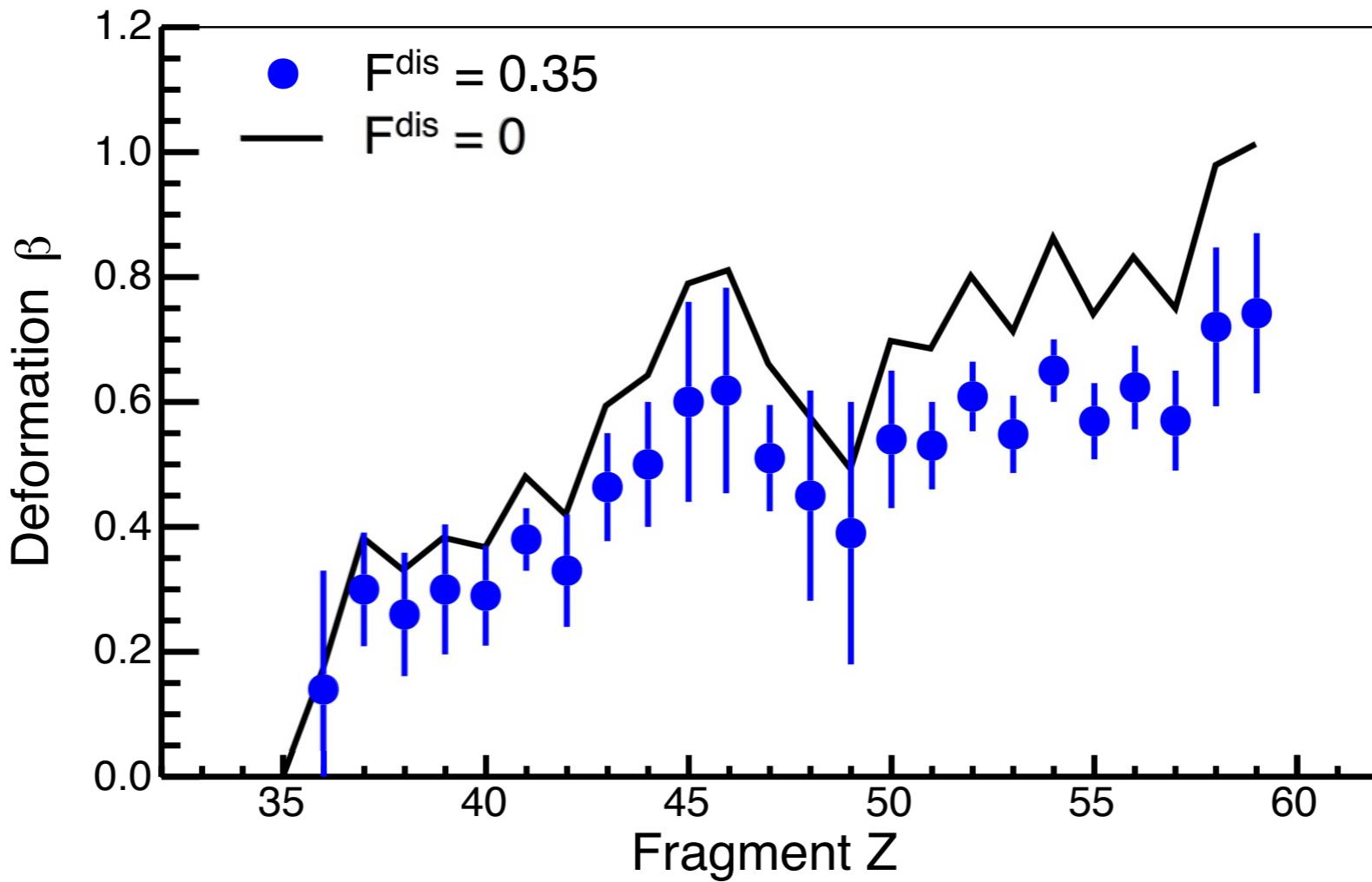
$$E_i^{*,\text{def}}(\beta_i) \approx (1 - F^{\text{dis}})(TXE - 3) \left( \frac{Q_i^\nu}{Q_1^\nu + Q_2^\nu} \right)$$

The value of  $F^{\text{dis}}$  is a weak point in our calculations, however, with  $F^{\text{dis}} = 0$  we have an upper limit for the fragment deformation.

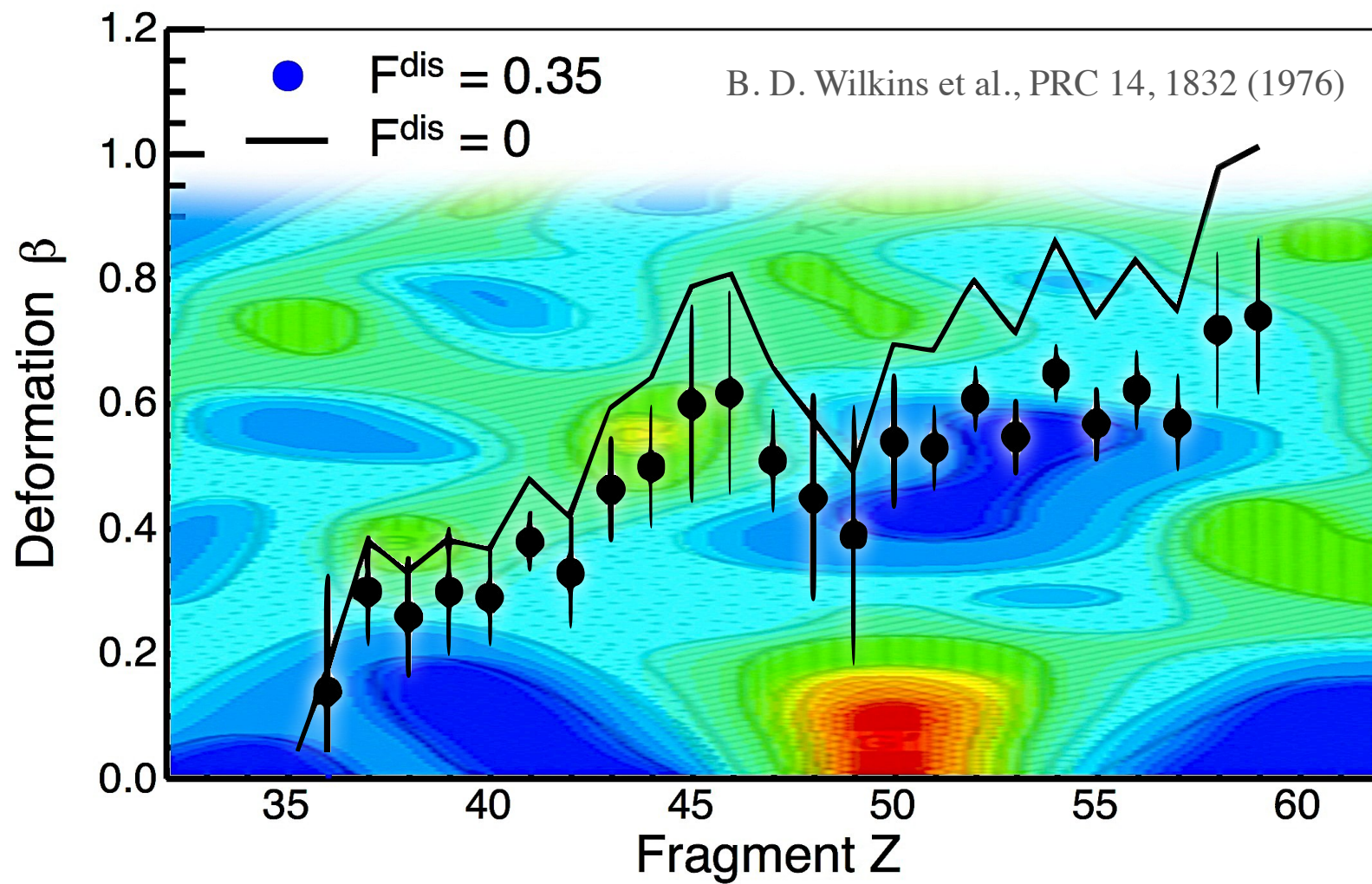


A. Bulgac et al., PRL 116, 122504 (2016)

## Deformation

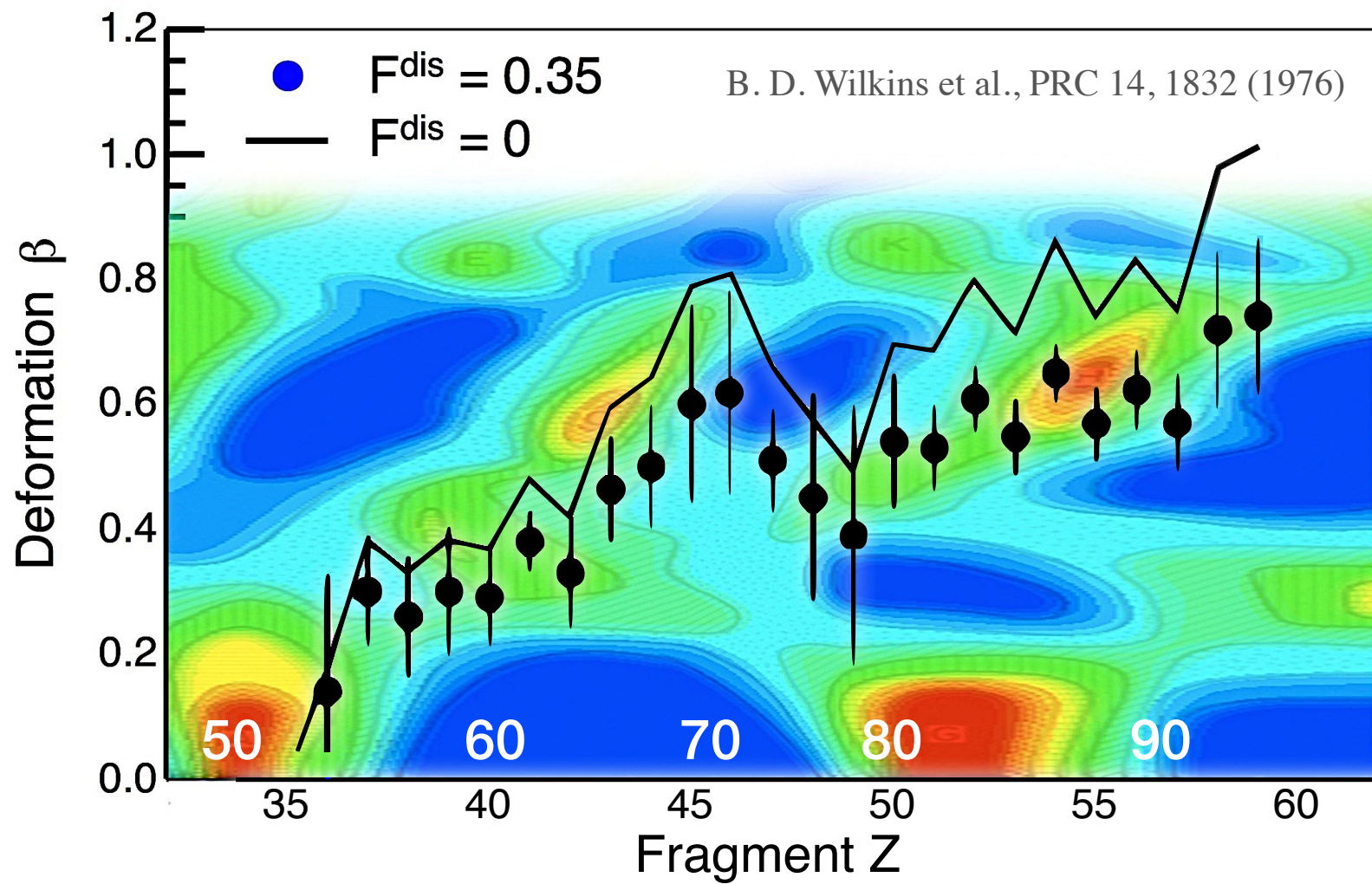


- The overall deformation is around 0.5
- The deformation grows with the size of the fragment, except between  $Z=45 - 50$ , reproducing the saw-tooth behaviour of the neutron multiplicity
- A minimum is formed around  $Z=50$ , but relatively far from spherical



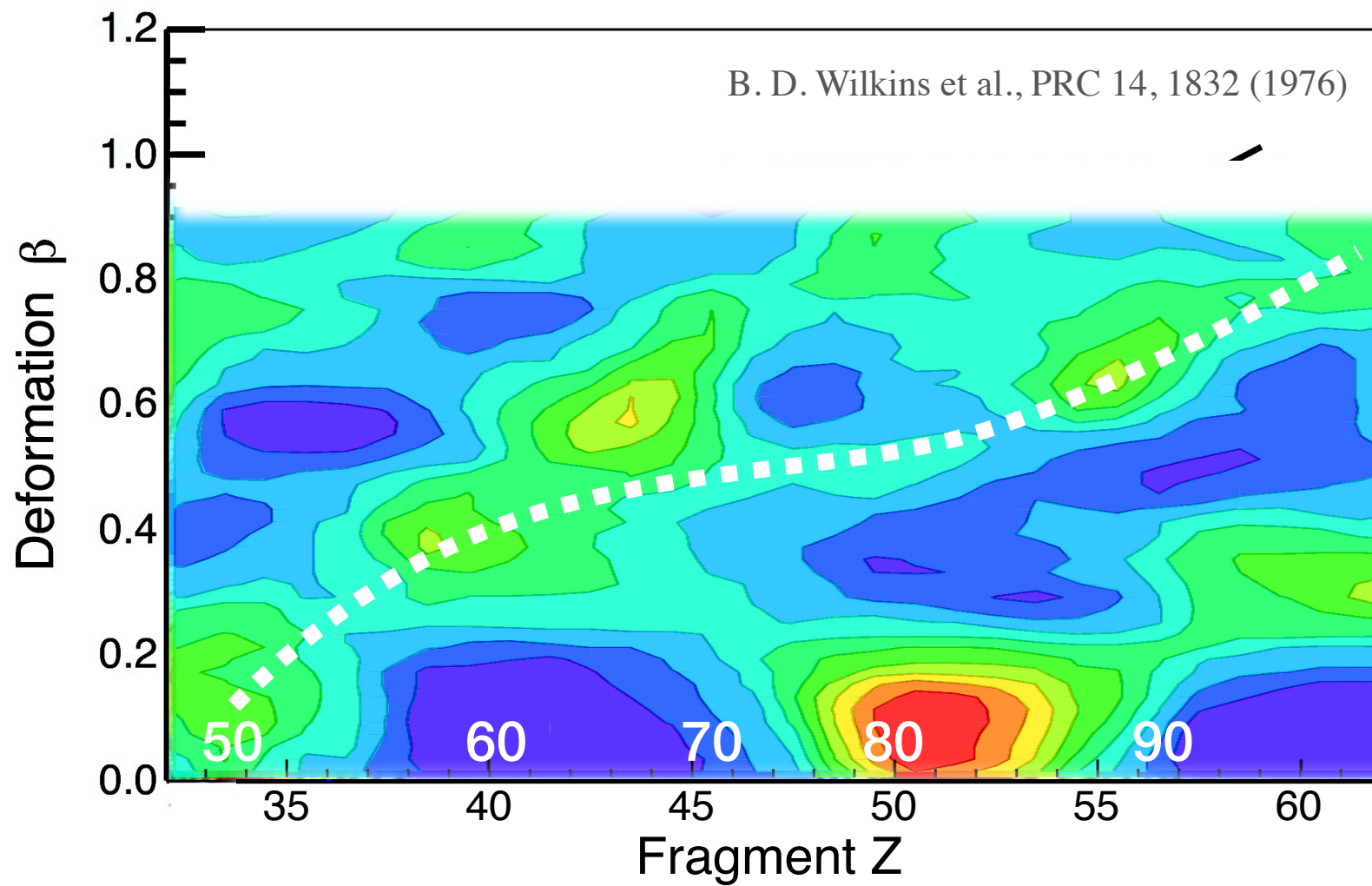
Energy correction to deformed proton shells

- Light fragments go through a weak minimum around  $Z=44$
- Around  $Z=50$ , the deformation seems to be dragged to the spherical configuration, but blocked by a “wall”.



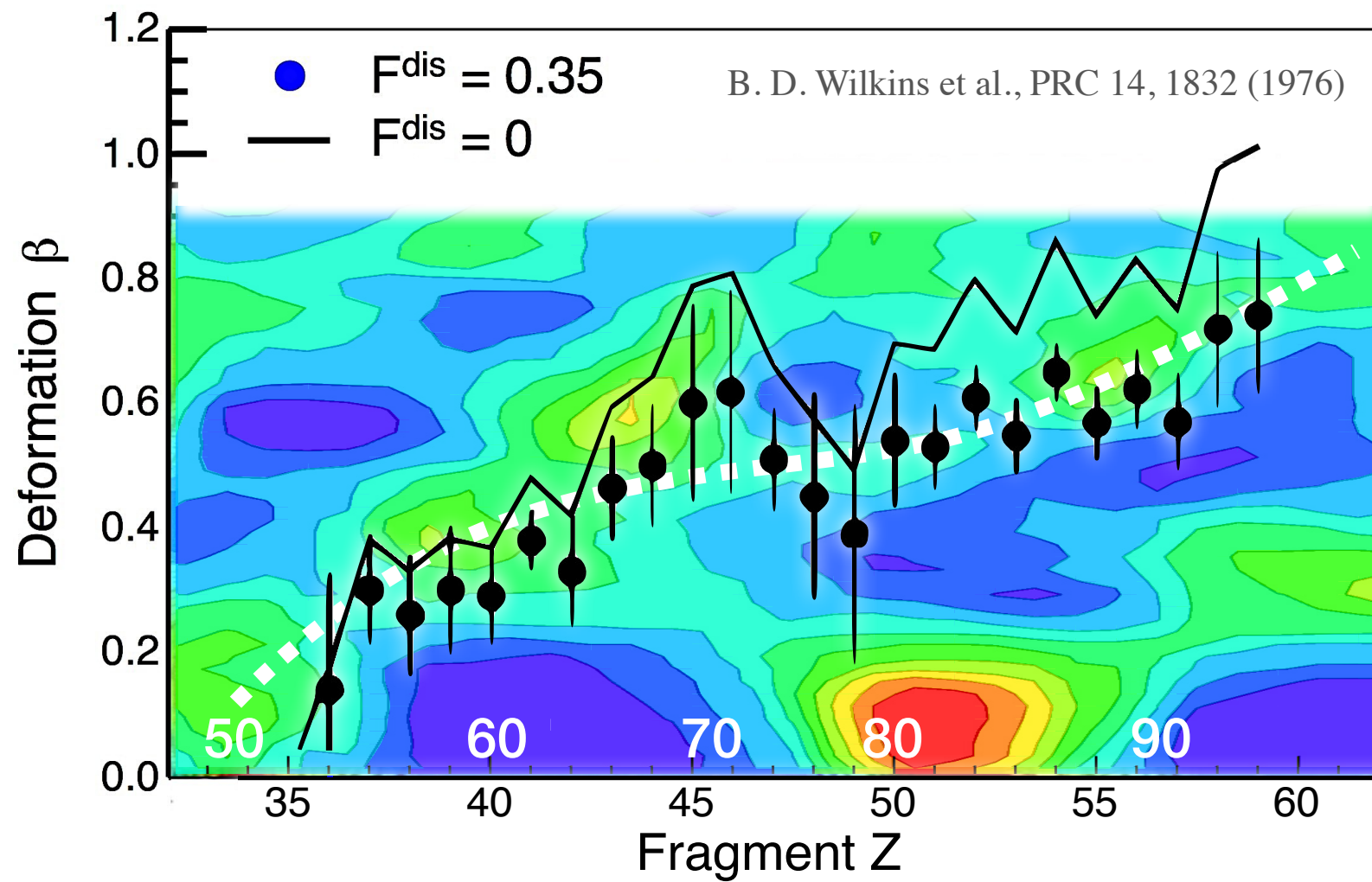
Energy correction to deformed neutron shells

- Light fragments run through a corridor with local minima at N=50 and 64
- Heavy fragments also run through a corridor with a minimum at N=88
- The deformation hardly approaches spherical configurations and the effect of N=82 seems weak, in this case.



Energy correction to deformed proton and neutron shells

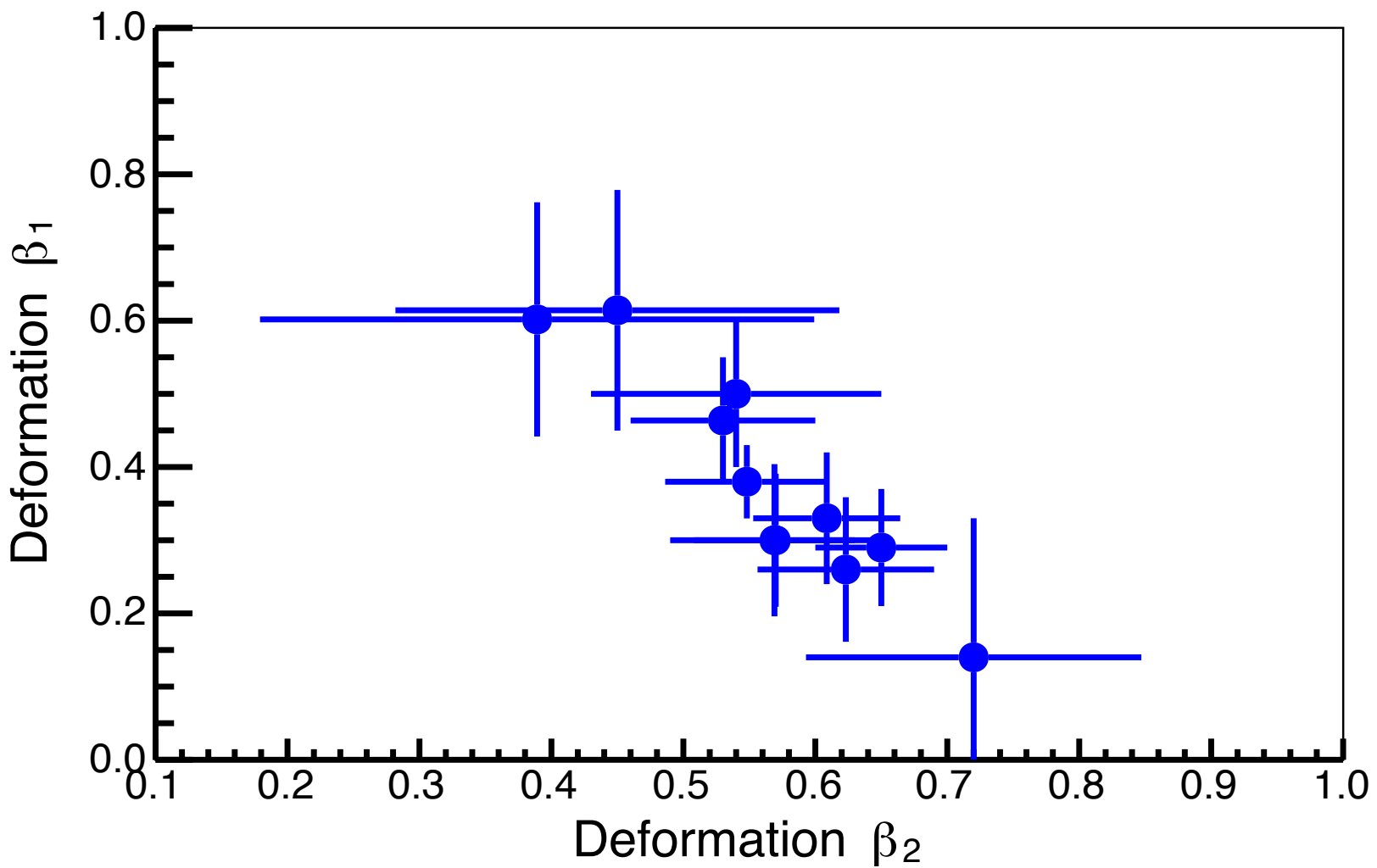
- When considered together, the corrections to n and p shells weakens the effect of N~88 and some of N~64.
- The N~64 remains as an accessible minimum out of what seems a long corridor.



Energy correction to deformed proton and neutron shells

- The experimental deformations mostly run through this corridor except around  $N \sim 64$ , where the approaching of the light fragment competes with the potential wall that its heavy partner finds at  $N \sim 80$ .

## Deformation. Correlation

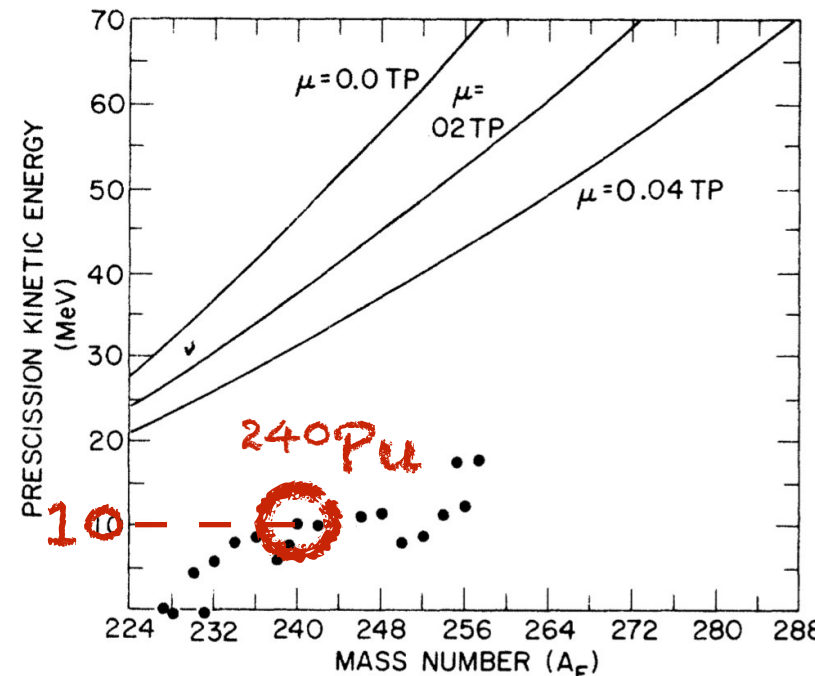


- We also realised there is a strong correlation between the deformation of split partners.

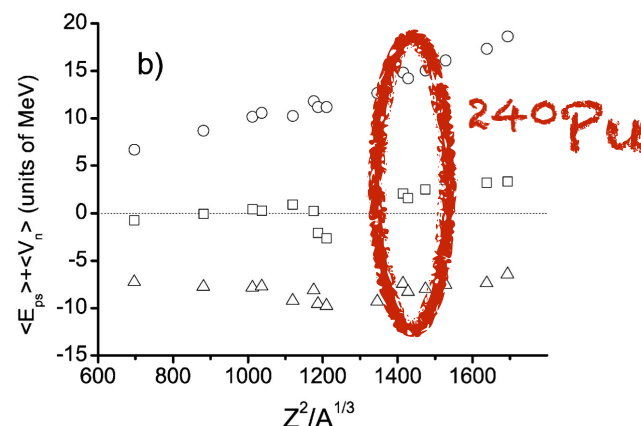
# Energy balance at scission. Kinetic energy

*measured*

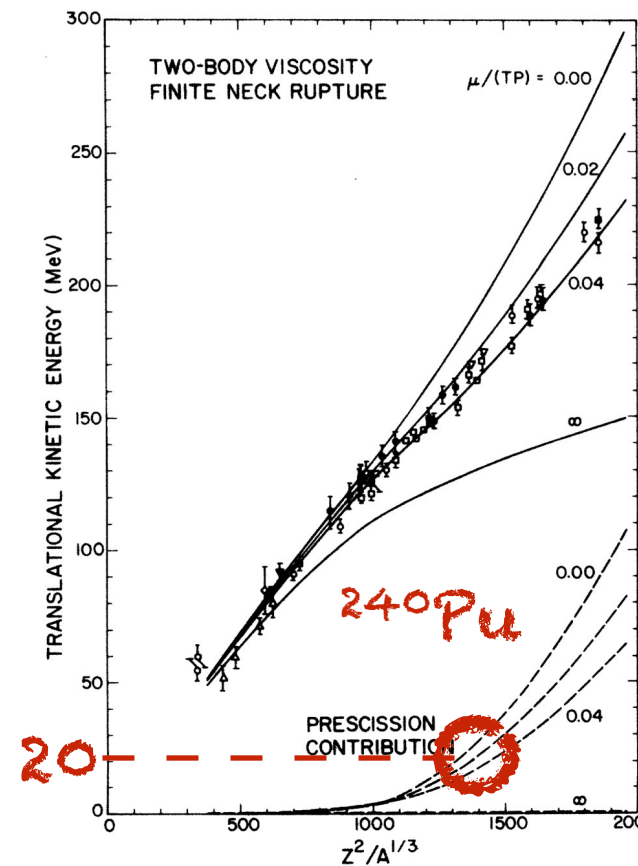
$$TKE = E^{k,C}(Z_1, Z_2, \beta_1, \beta_2, d) + E^{k,pre}$$



B. D. Wilkins et al., PRC 14, 1832 (1976)

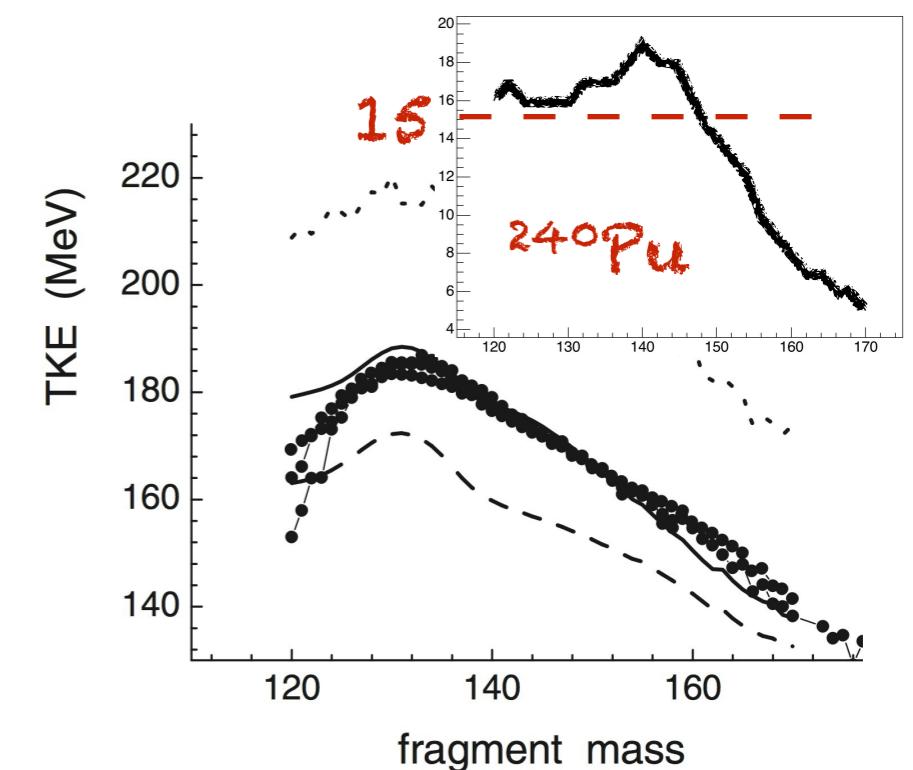


M. Borunov et al., NPA 799, 56 (2008)



K. Davies et al., PRC 16, 1890 (1977)

pre-scission  
energy



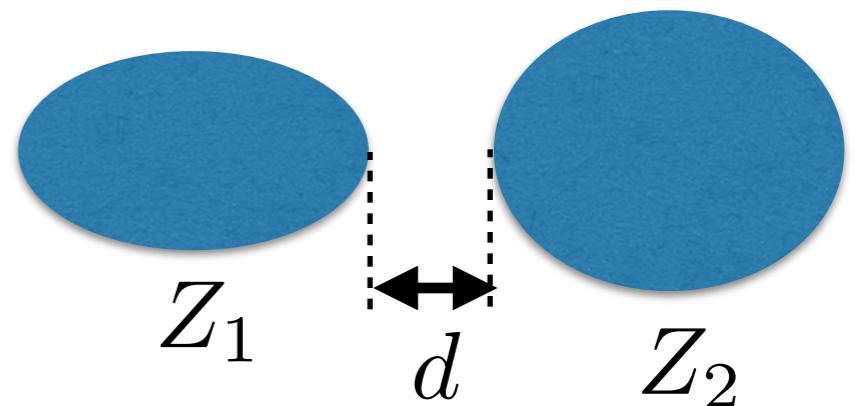
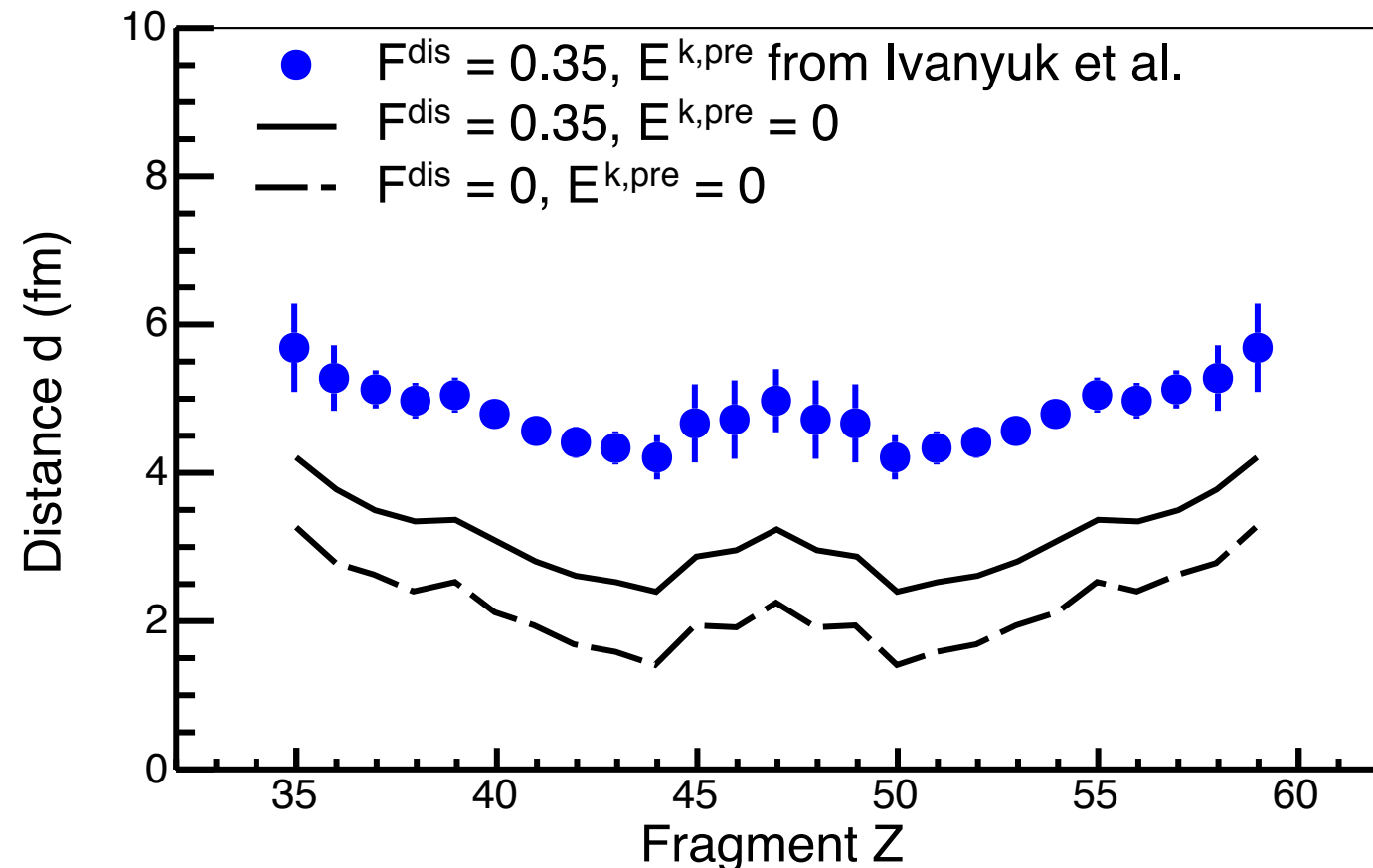
F. Ivanyuk et al., PRC 90, 054607 (2014)

Different models estimate it between 10-20 MeV.  
We will use the calculations of Ivanyuk et al.

# Energy balance at scission. Tip distance

$$E^{k,C}(Z_1, Z_2, \beta_1, \beta_2, d) = \text{TKE} - E_{\text{Ivanyuk}}^{\text{k,pre}}$$

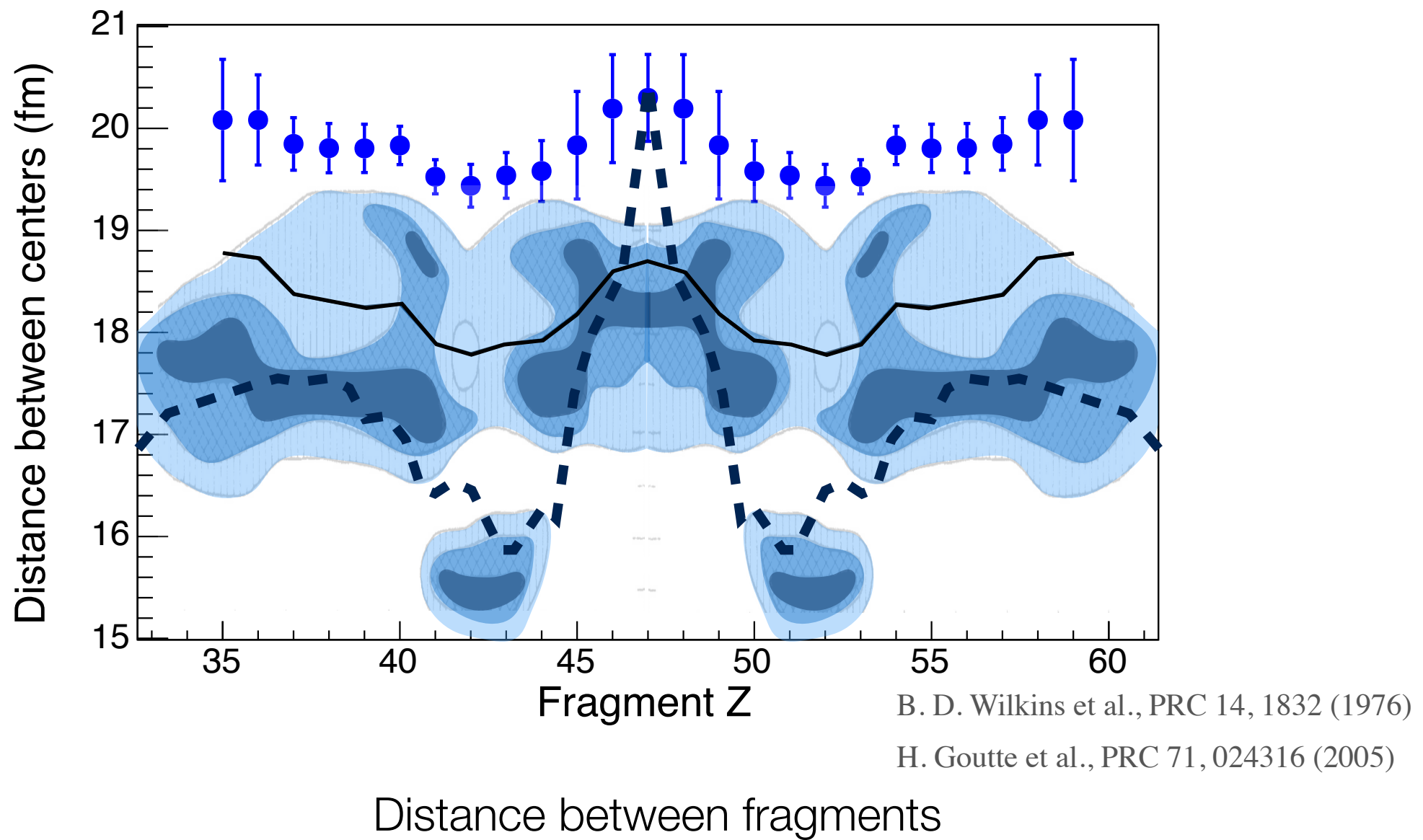
measured



We use the formula of Cohen-Swiatecki to calculate the repulsion between two coaxial homogeneously charged ellipsoids

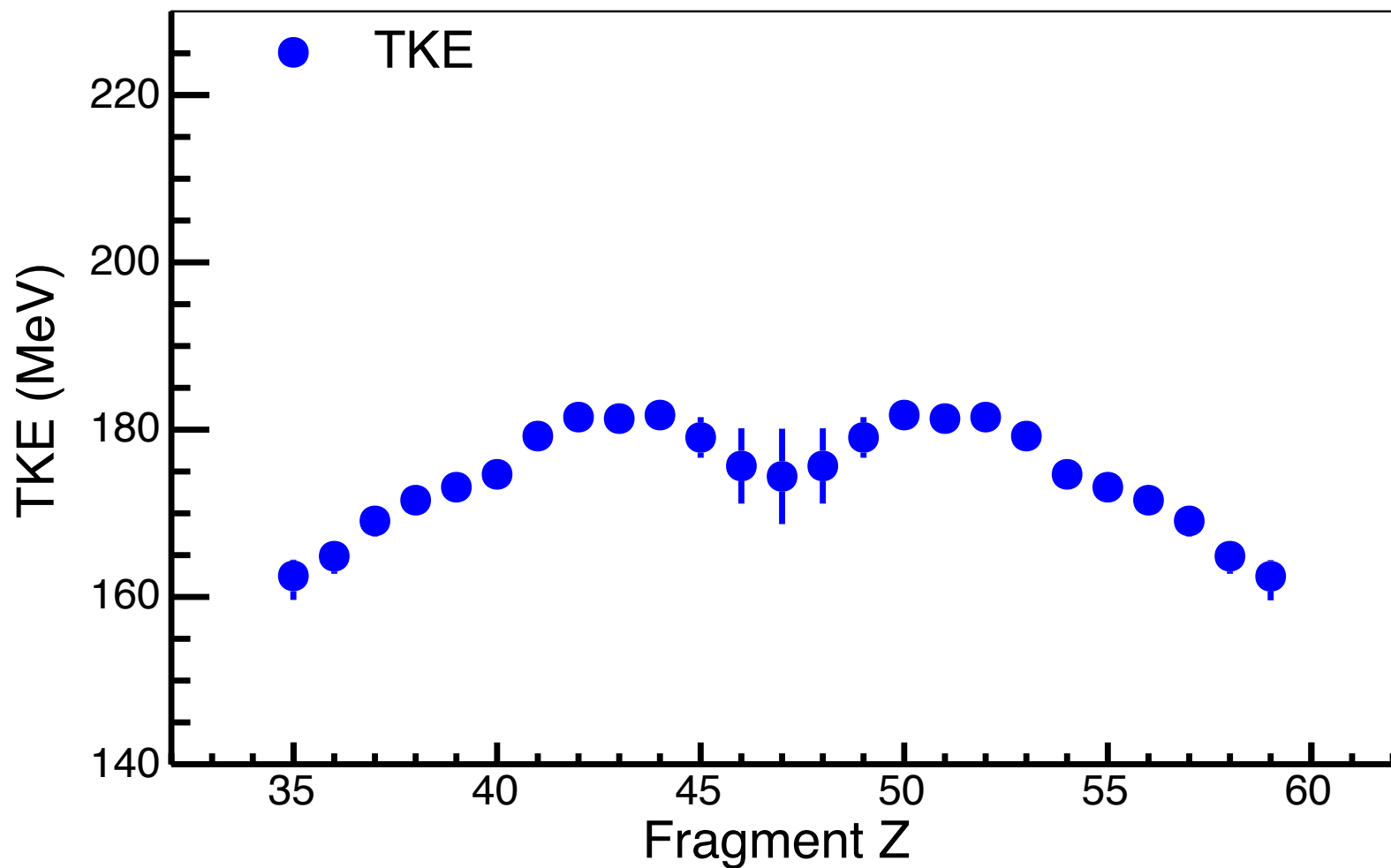
S. Cohen and W. Swiatecki, Annals of Physics  
19, 67 (1962).

- The overall value is  $\sim 5$  fm, which is much larger than the “standard” (below 3 fm). Only at the lower limit reaches  $\sim 2$  fm.
- A distinctive minimum appears at  $Z=50$ .

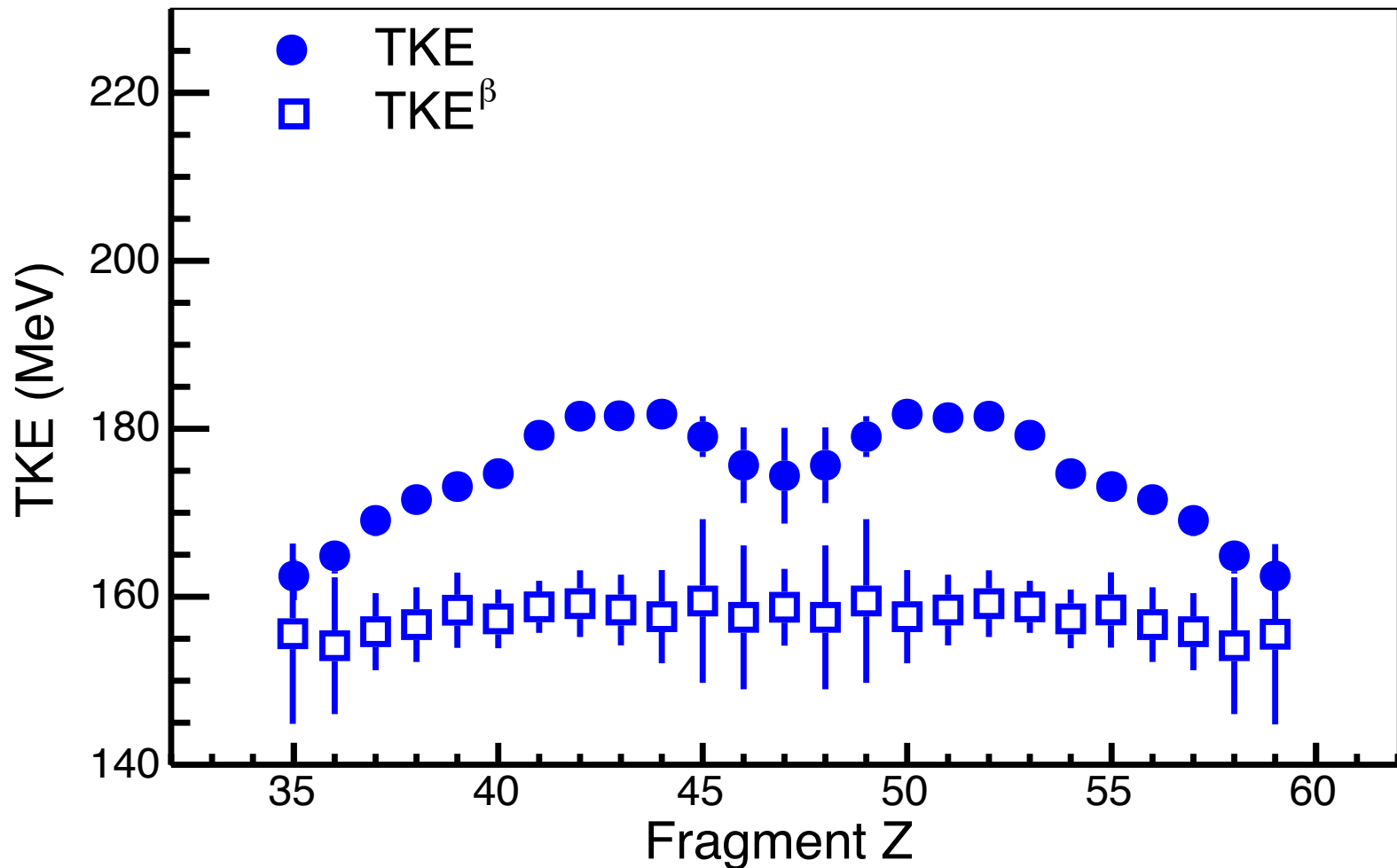


- SPM calculations for  $^{236}\text{U}$  also predict a minimum around  $Z \sim 52$ . Although more pronounced. HFB calculations also calculate a deeper minimum around  $Z \sim 52$  for  $^{238}\text{U}$

TKE, who decides its shape?

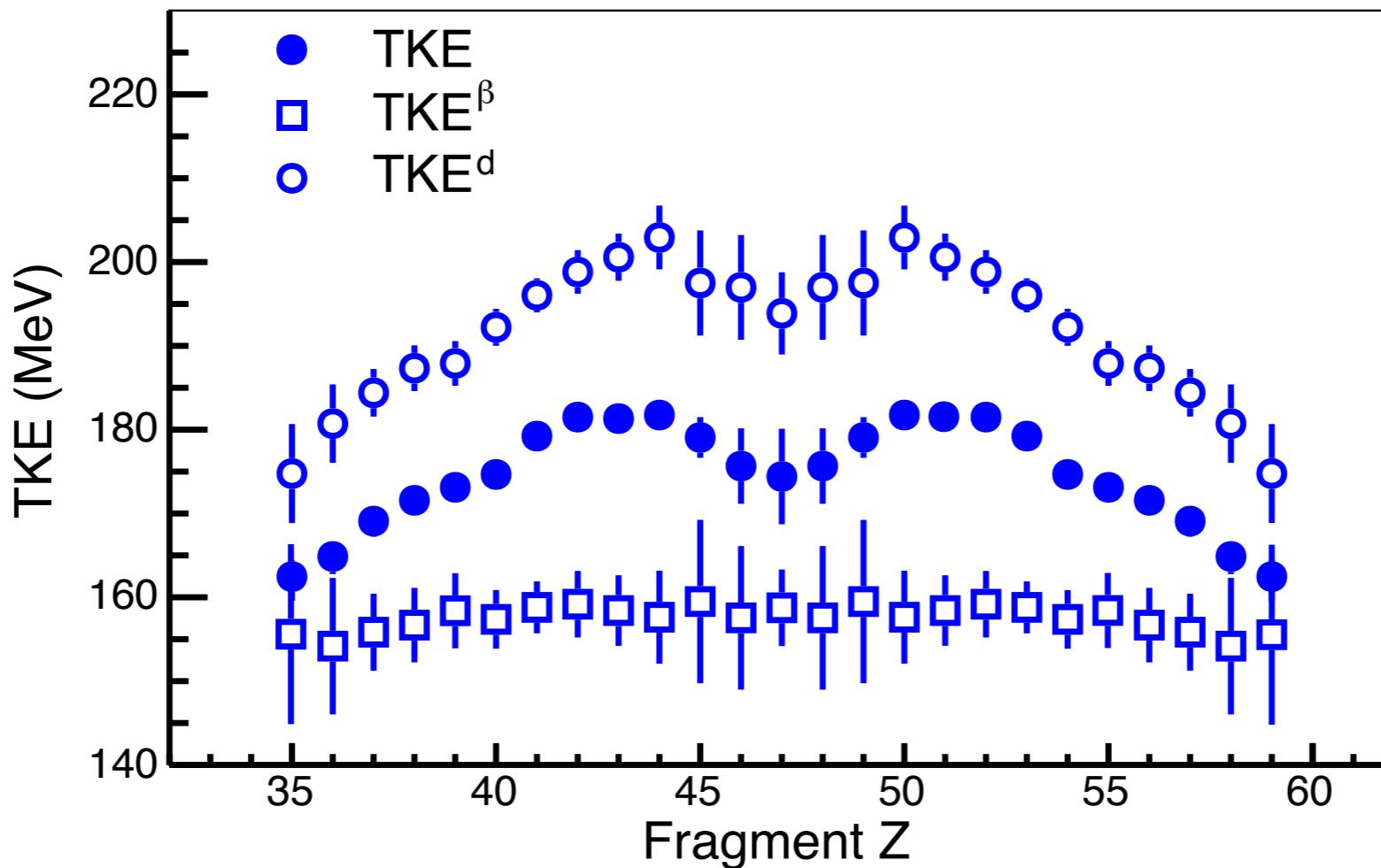


TKE, who decides its shape?



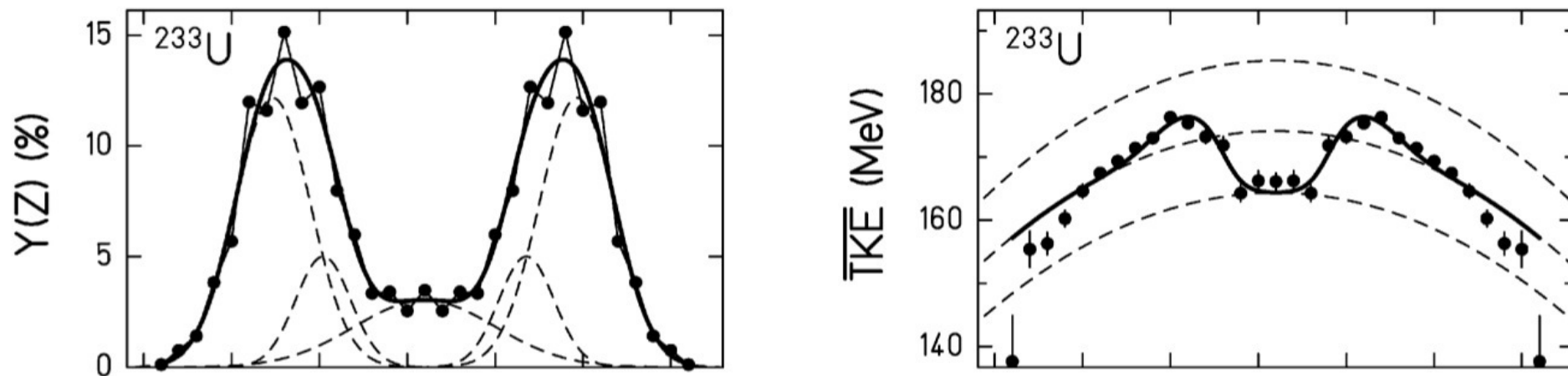
- Fixing the tip distance, the effect of the deformation alone does not reproduce the features of the observed TKE.

# TKE, who decides its shape?



- Fixing the tip distance, the effect of the deformation alone does not reproduce the features of the observed TKE.
- The effect of the neck distribution applied to spherical fragments mimics the same behaviour of the TKE.
- There must be a mechanism that links the structure effects to the length of the neck.

C. Böckstiegel et al. / Nuclear Physics A 802 (2008) 12–25



Assuming  $\beta$  and  $d$  are unique for each mode, we fit simultaneously the isotopic yield distribution and the TKE

$$Y_Z = \sum_j \frac{I_j}{\sigma_j \sqrt{2\pi}} \exp \left( \frac{-(Z - Z_{0,j})^2}{2\sigma_j^2} \right)$$

$$TKE_Z = \frac{\sum_j Y_Z(Z_{0,j}, \sigma_j, I_j) \cdot E^{k,C}(\beta_{1,j}, \beta_{2,j}, d_j)}{\sum_j Y_Z(Z_{0,j}, \sigma_j, I_j)} + E^{k,pre}$$

# Fission modes

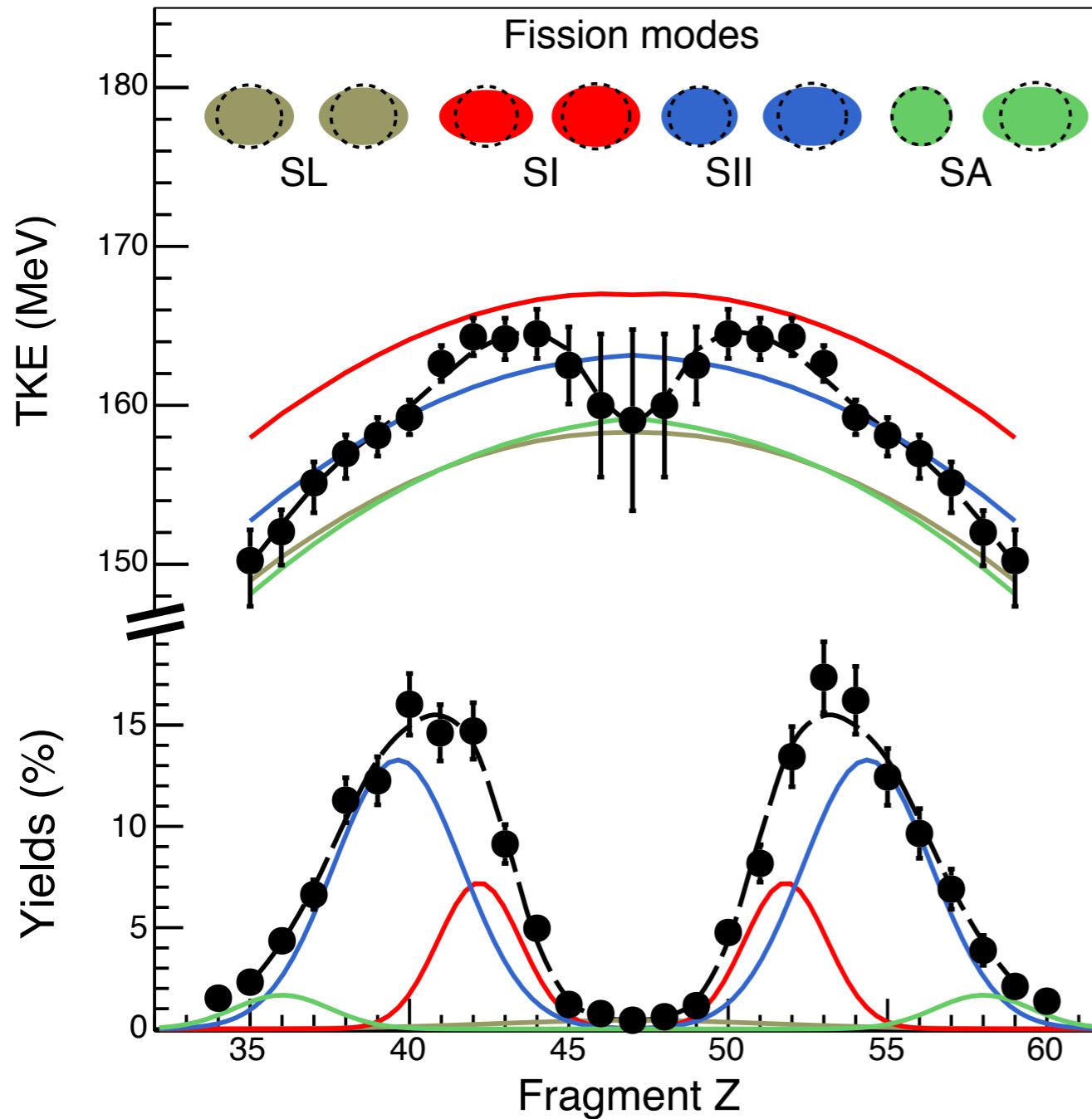


TABLE I. Fission channel parameters.

|                 | SL      | SI      | SII     | SA     |
|-----------------|---------|---------|---------|--------|
| $Z_0$           | 47      | 51.8(4) | 54.4(4) | 58(2)  |
| $\sigma$        | 4.4(4)  | 1.3(2)  | 2.0(1)  | 1.5(2) |
| Yield (%)       | 5(1)    | 23(8)   | 66(9)   | 6(3)   |
| $\beta_1$       | 0.5(1)  | 0.7(2)  | 0.3(1)  | 0.0(2) |
| $\beta_2$       | 0.5(1)  | 0.4(1)  | 0.6(1)  | 0.7(4) |
| $d$ (fm)        | 4.9(3)  | 3.8(4)  | 4.9(2)  | 5.9(7) |
| $R_{c.m.}$ (fm) | 20.4(6) | 19.3(6) | 19.8(6) | 20(1)  |

- The modes on the yield distribution are pretty much in agreement with previous measurements
- We find a super-asymmetric component with similar contribution as that of the super-long mode.

# Fission modes

B. D. Wilkins et al., PRC 14, 1832 (1976)

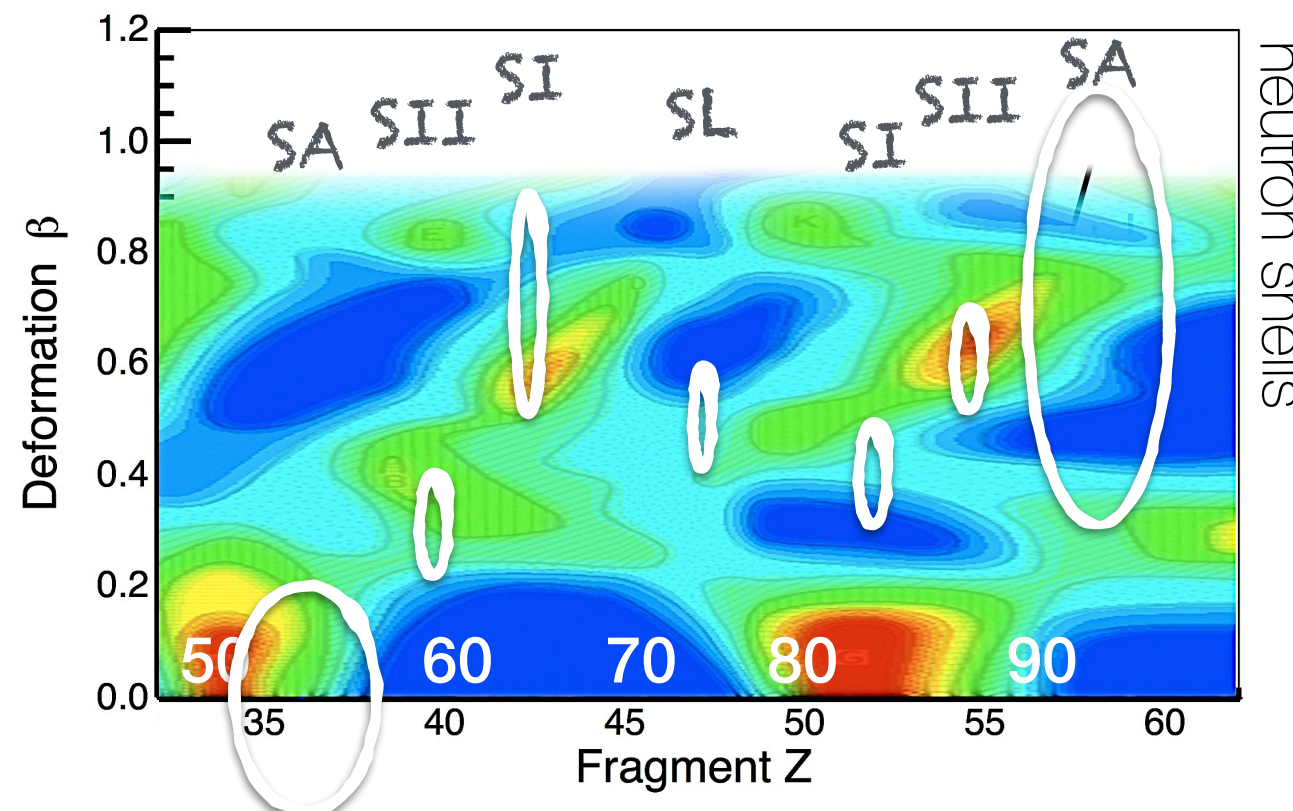


TABLE I. Fission channel parameters.

|                 | SL      | SI      | SII     | SA     |
|-----------------|---------|---------|---------|--------|
| $Z_0$           | 47      | 51.8(4) | 54.4(4) | 58(2)  |
| $\sigma$        | 4.4(4)  | 1.3(2)  | 2.0(1)  | 1.5(2) |
| Yield (%)       | 5(1)    | 23(8)   | 66(9)   | 6(3)   |
| $\beta_1$       | 0.5(1)  | 0.7(2)  | 0.3(1)  | 0.0(2) |
| $\beta_2$       | 0.5(1)  | 0.4(1)  | 0.6(1)  | 0.7(4) |
| $d$ (fm)        | 4.9(3)  | 3.8(4)  | 4.9(2)  | 5.9(7) |
| $R_{c.m.}$ (fm) | 20.4(6) | 19.3(6) | 19.8(6) | 20(1)  |

- SL: Is “stuck” between two walls
- SI: N~64 decides the deformation on the light fragment
- SII: N~88 decides the deformation on the heavy fragment
- SA: Might be dragging its light fragment towards N=50

# Fission modes

B. D. Wilkins et al., PRC 14, 1832 (1976)

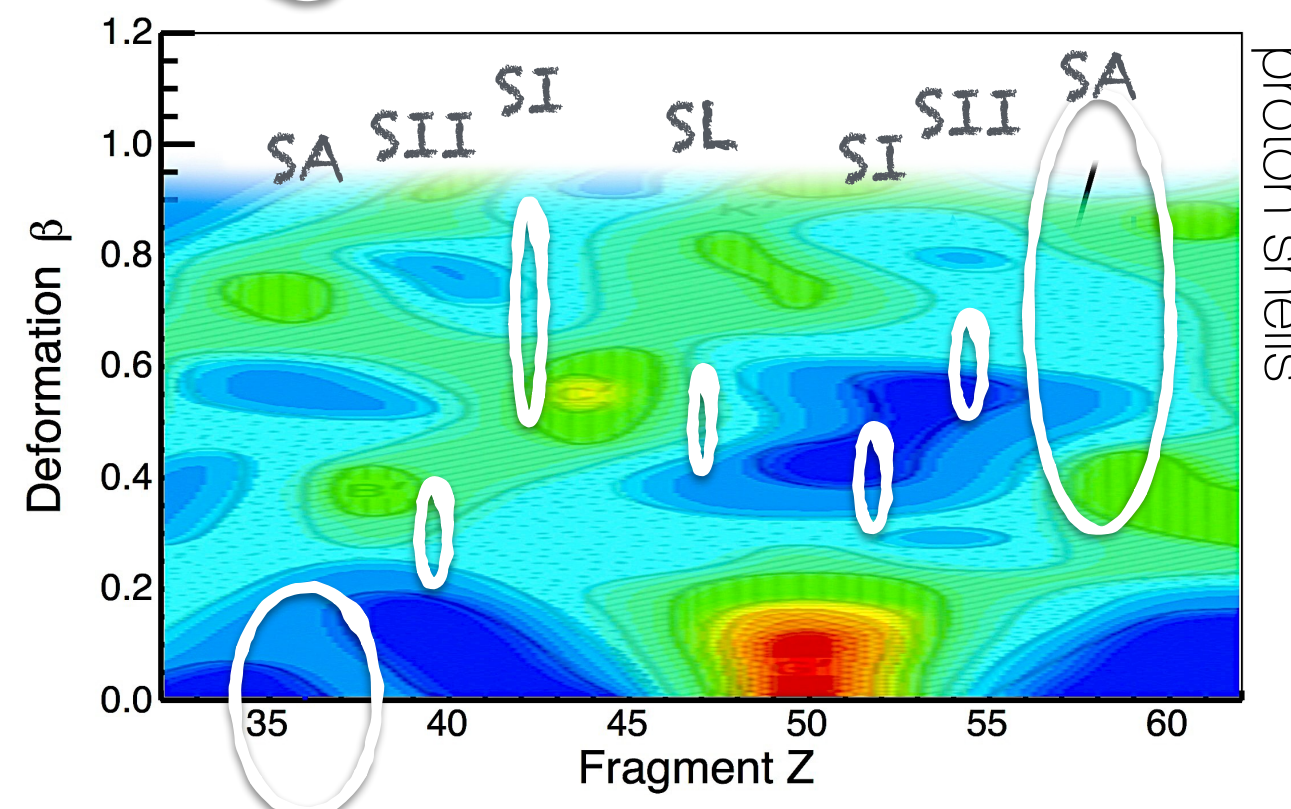
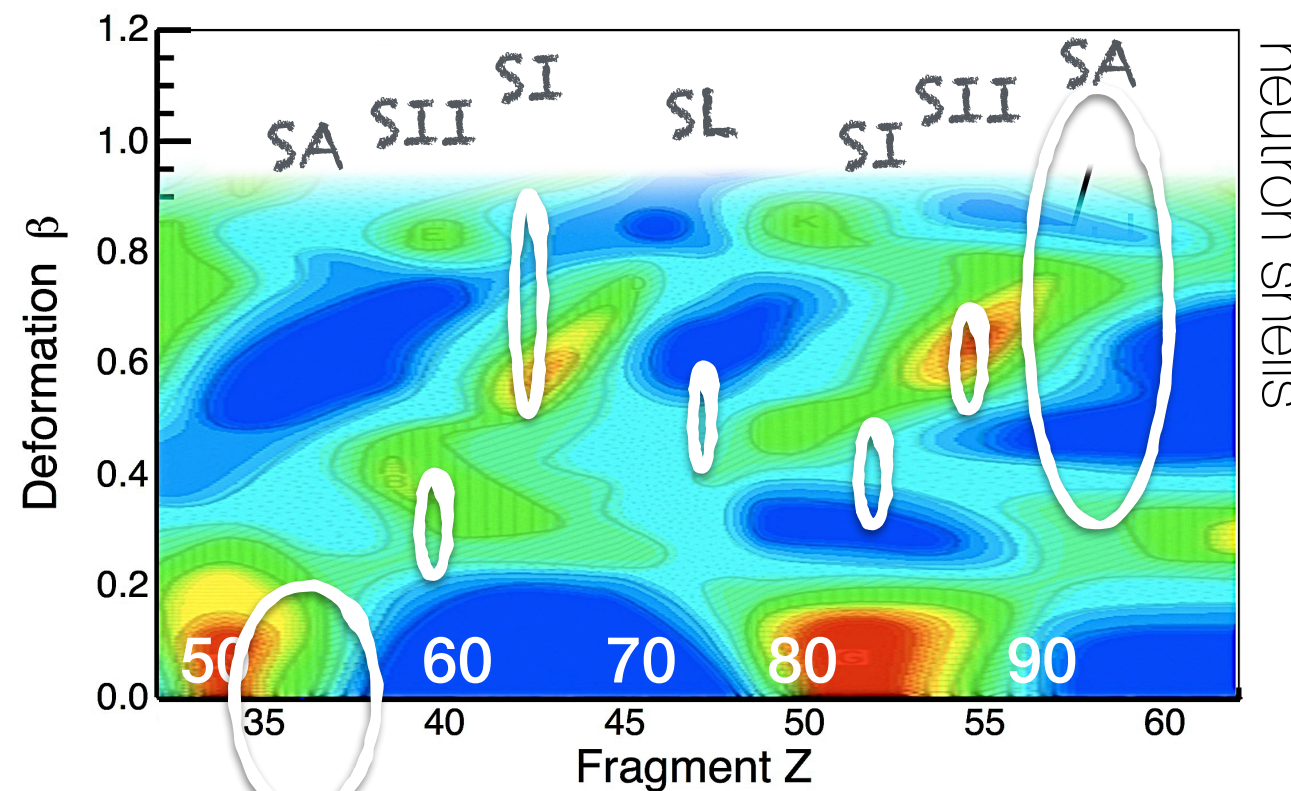


TABLE I. Fission channel parameters.

|                 | SL      | SI      | SII     | SA     |
|-----------------|---------|---------|---------|--------|
| $Z_0$           | 47      | 51.8(4) | 54.4(4) | 58(2)  |
| $\sigma$        | 4.4(4)  | 1.3(2)  | 2.0(1)  | 1.5(2) |
| Yield (%)       | 5(1)    | 23(8)   | 66(9)   | 6(3)   |
| $\beta_1$       | 0.5(1)  | 0.7(2)  | 0.3(1)  | 0.0(2) |
| $\beta_2$       | 0.5(1)  | 0.4(1)  | 0.6(1)  | 0.7(4) |
| $d$ (fm)        | 4.9(3)  | 3.8(4)  | 4.9(2)  | 5.9(7) |
| $R_{c.m.}$ (fm) | 20.4(6) | 19.3(6) | 19.8(6) | 20(1)  |

- SL: Is “stuck” between two walls
- SI:  $N \sim 64$  decides the deformation on the light fragment
- SII:  $N \sim 88$  decides the deformation on the heavy fragment
- SA: Might be dragging its light fragment towards  $N=50$
- Proton shells seem to have little influence, except, maybe, at SI ( $Z \sim 44$ )

# Fission modes

B. D. Wilkins et al., PRC 14, 1832 (1976)

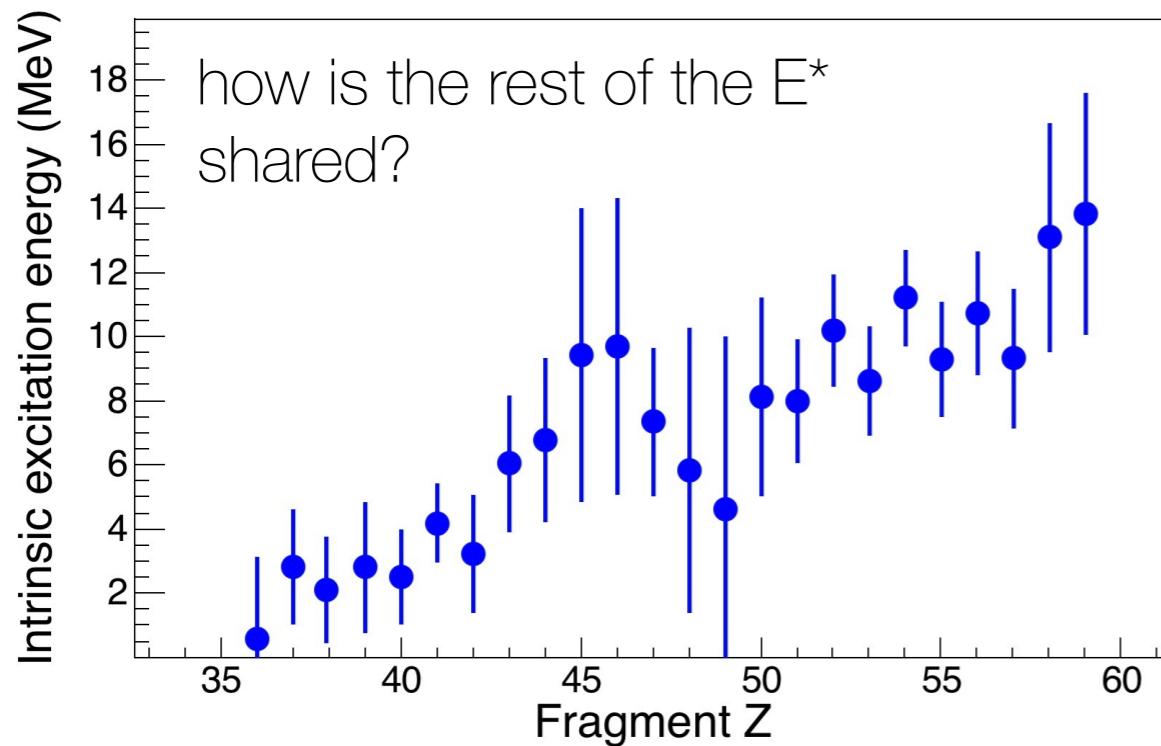
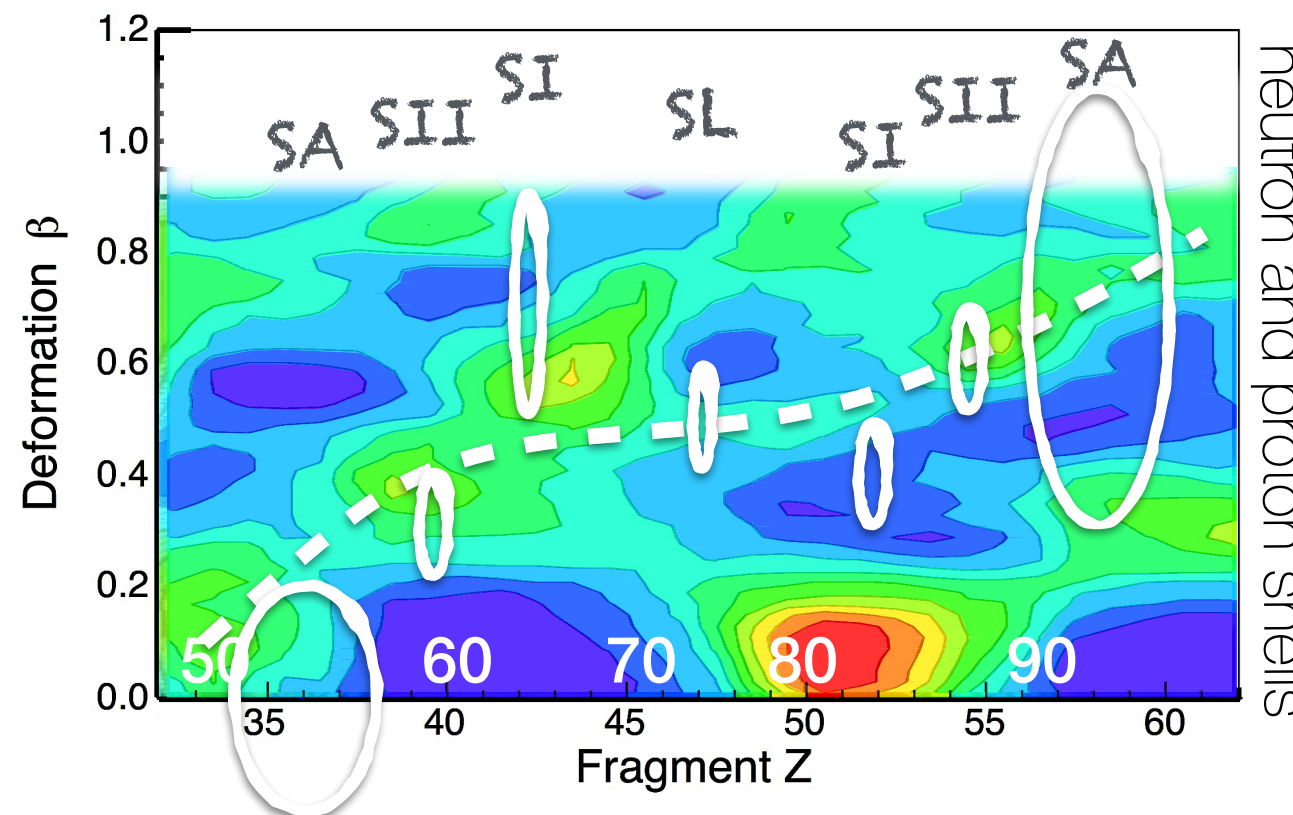


TABLE I. Fission channel parameters.

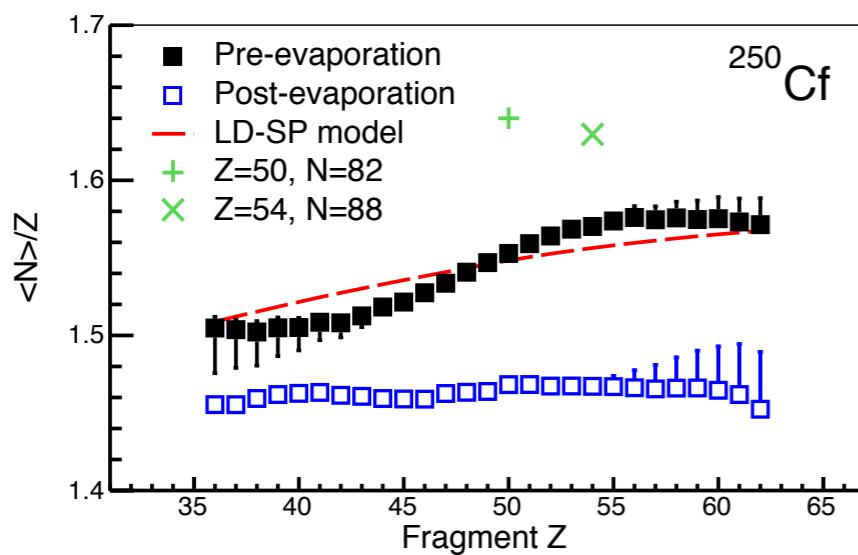
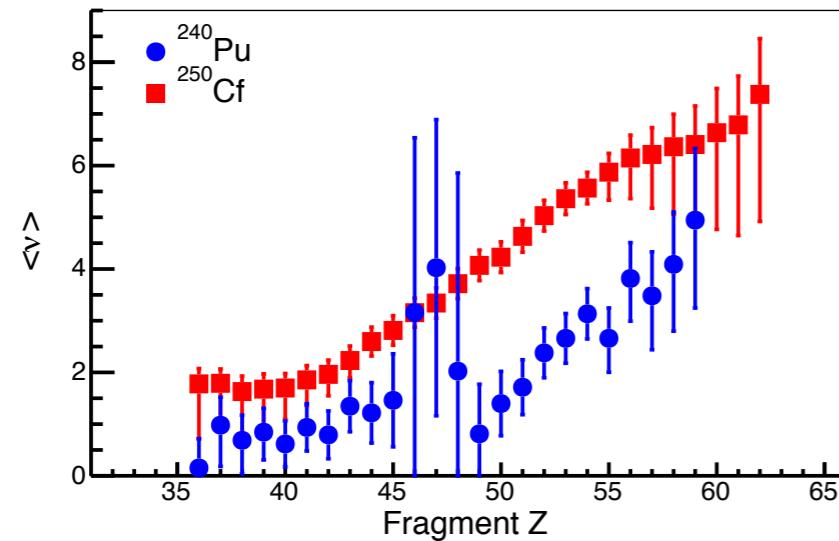
|                 | SL      | SI      | SII     | SA     |
|-----------------|---------|---------|---------|--------|
| $Z_0$           | 47      | 51.8(4) | 54.4(4) | 58(2)  |
| $\sigma$        | 4.4(4)  | 1.3(2)  | 2.0(1)  | 1.5(2) |
| Yield (%)       | 5(1)    | 23(8)   | 66(9)   | 6(3)   |
| $\beta_1$       | 0.5(1)  | 0.7(2)  | 0.3(1)  | 0.0(2) |
| $\beta_2$       | 0.5(1)  | 0.4(1)  | 0.6(1)  | 0.7(4) |
| $d$ (fm)        | 4.9(3)  | 3.8(4)  | 4.9(2)  | 5.9(7) |
| $R_{c.m.}$ (fm) | 20.4(6) | 19.3(6) | 19.8(6) | 20(1)  |

- Mostly, all the modes have configurations around 20 fm, except the SI.
- As we saw previously, the SI mode: is the only deviation from a long corridor.
- Also, more nucleons “blocked” in shells and less on the neck, making it “brittle”? Is this the connection between shells and TKE?

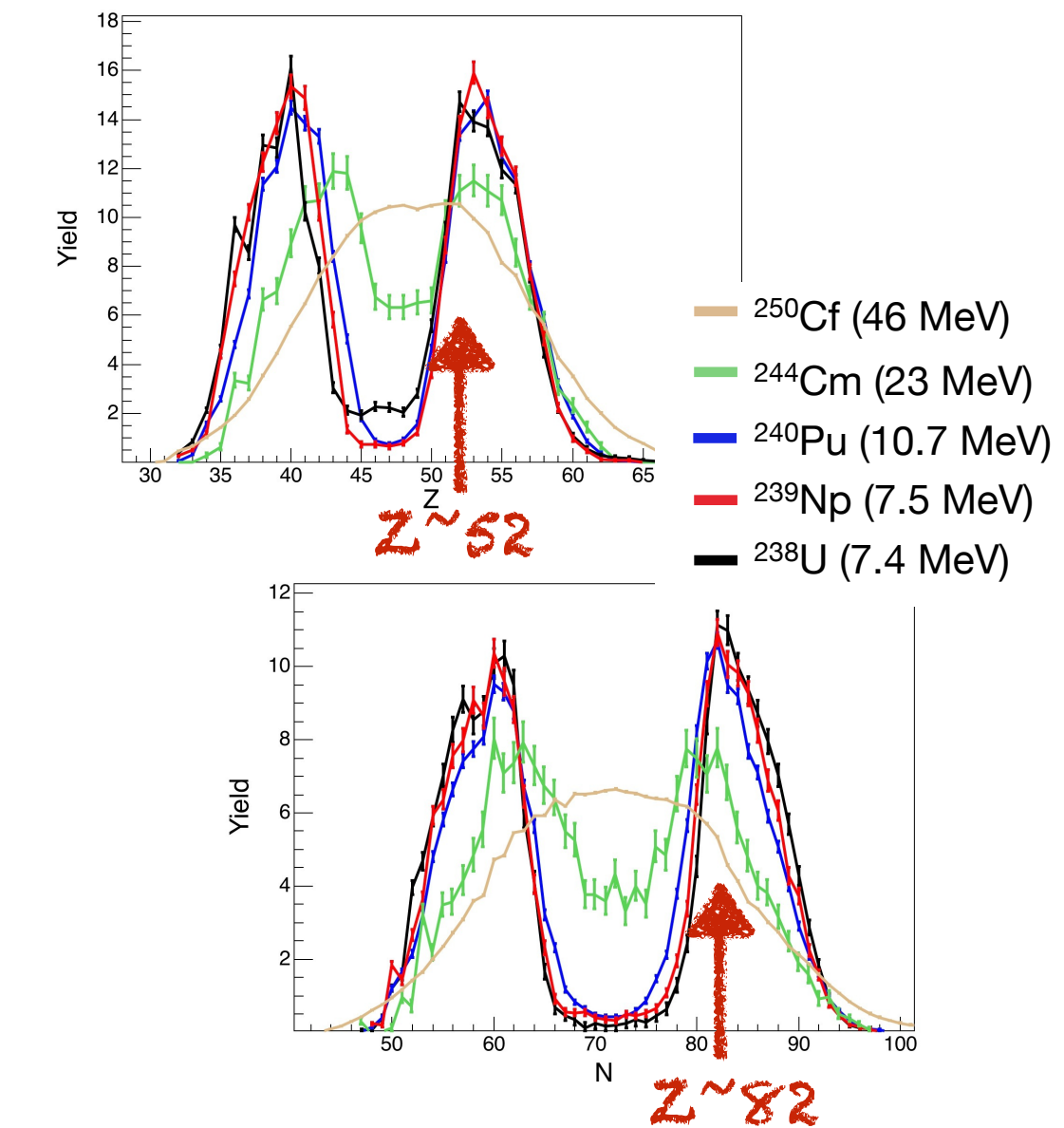
## Wrap up

- The calculation of TKE, TXE, neutron multiplicity, and neutron excess at scission was possible with the measurement of the fragments yield, velocity, and as a function of the fragment identification in ( $Z, A$ ).
- A detailed energy balance at scission with these observables allowed us to estimate the deformation and separation of the emerging fragments.
- The results show that mostly deformed neutron shells are responsible for the fragment deformation.
- The link between these shell effects and the measured TKE is done through the tip distance, hinting at a direct link between structure and the length of the neck.

Next



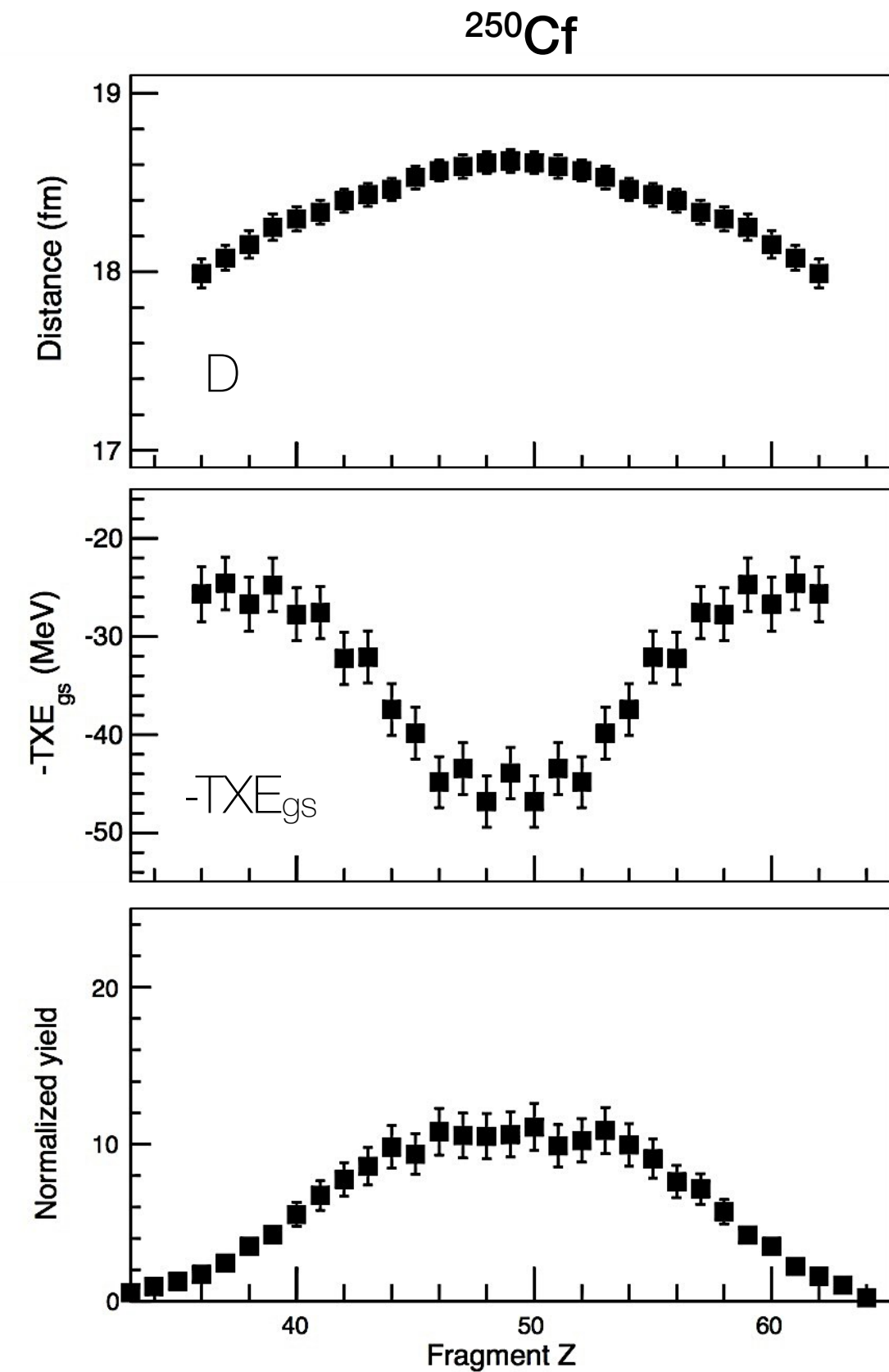
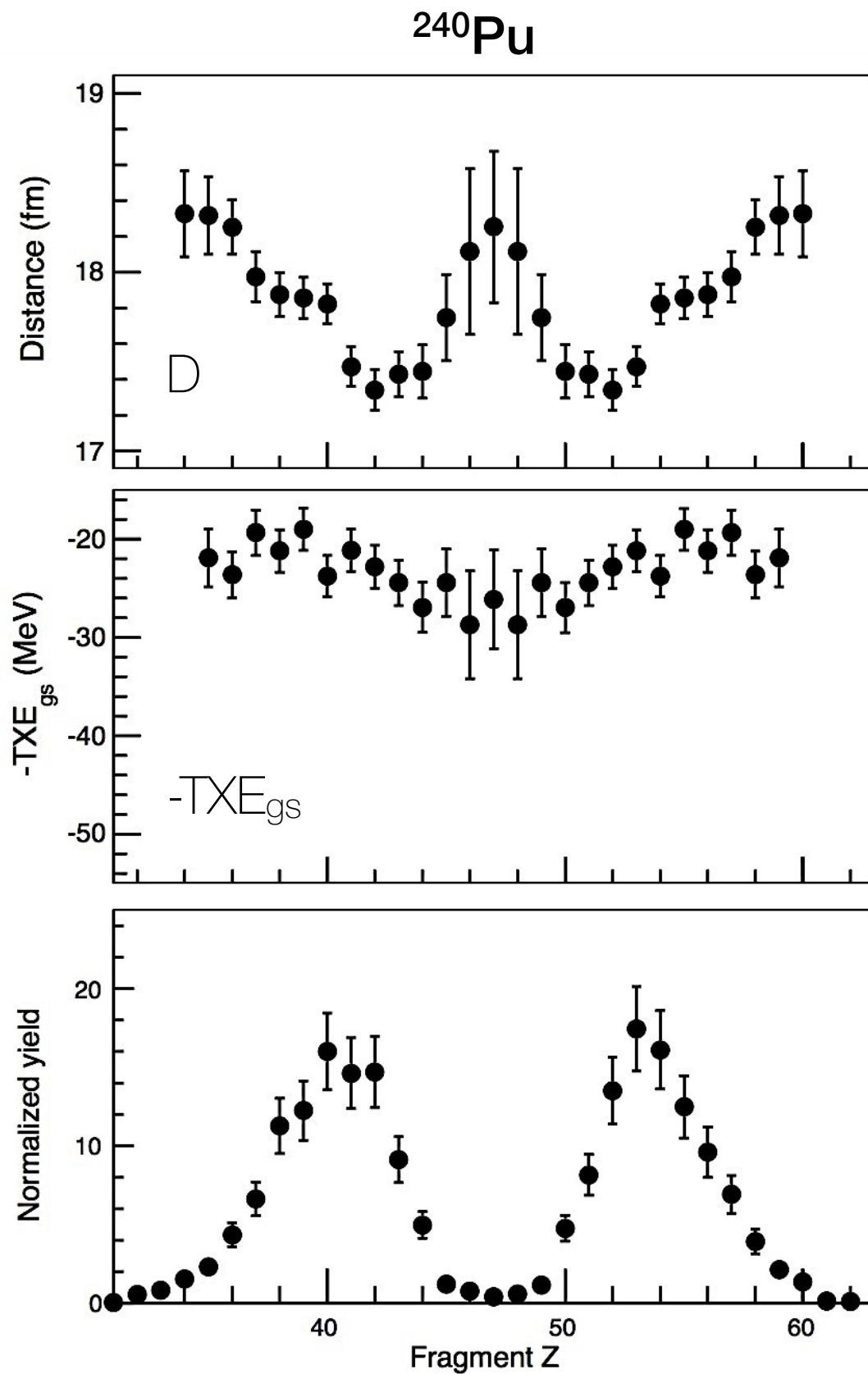
- Investigate the deformation of  $^{250}\text{Cf}$  at 42 MeV and its mysterious N/Z



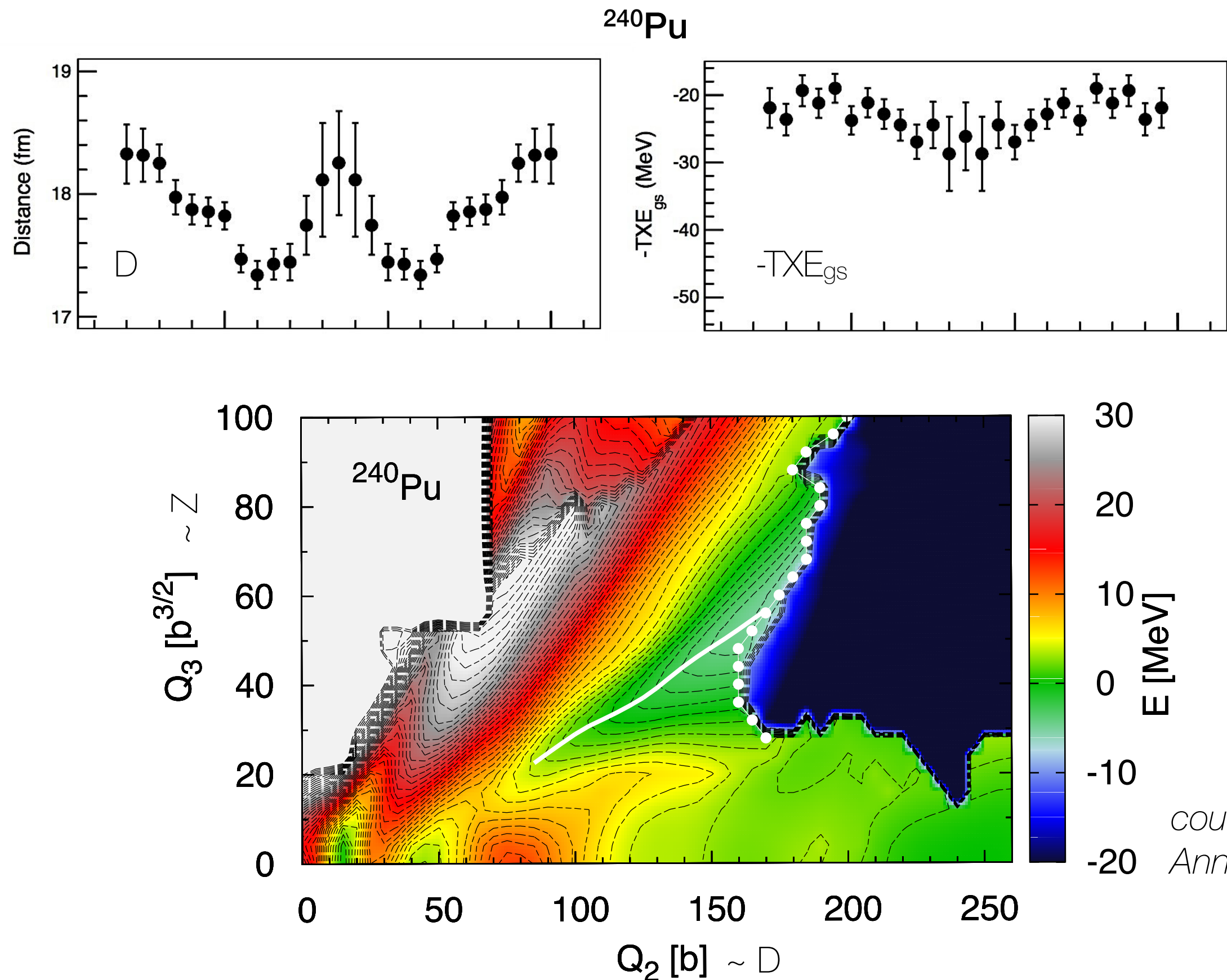
- Study the systematics of Diego's data as a function of  $E^*$



# Scission landscape



# Scission landscape



# Scission landscape

